


Spring 2018

Synthesis and Behavior Characterization of Multi-Scale Hierarchical Structured Composites

Jacob M. Mayfield

Follow this and additional works at: <https://digitalcommons.georgiasouthern.edu/etd>

 Part of the [Biology and Biomimetic Materials Commons](#), and the [Polymer and Organic Materials Commons](#)

Recommended Citation

Mayfield, Jacob M., "Synthesis and Behavior Characterization of Multi-Scale Hierarchical Structured Composites" (2018). *Electronic Theses and Dissertations*. 1766.
<https://digitalcommons.georgiasouthern.edu/etd/1766>

This thesis (open access) is brought to you for free and open access by the Graduate Studies, Jack N. Averitt College of at Digital Commons@Georgia Southern. It has been accepted for inclusion in Electronic Theses and Dissertations by an authorized administrator of Digital Commons@Georgia Southern. For more information, please contact digitalcommons@georgiasouthern.edu.

SYNTHESIS AND BEHAVIOR CHARACTERIZATION OF MULTI-SCALE HIERARCHICAL STRUCTURED COMPOSITES

by

JACOB MAYFIELD

(Under the Direction of Shaowen Xu)

ABSTRACT

The purpose of the synthesis of a multi-scale hierarchical composite material was to create a material with a high specific strength, a low mass, and high strength material. To achieve this the material categorization of the Formlabs Tough V2 resin was conducted. The resin was used in the construction of a biomimicry diamond lattice structure. The structure was subjected to compression testing to characterize the material properties. The Tough V2 resin structure combined with cellulose created a multi-scaled material on Macro and Micro levels to show the bio-inspired design to increase the material properties in a favorable manor. The Tough V2 material degrades by time and accounts for the irregularities in this research, and this was overcome using a control sample with the final product. A control and final product were tested producing results that proved the final product had an overall increase in materials properties. An increase in specific strength of 1.75 times with average control value of $0.0495 \text{ MPa}\cdot\text{m}^3/\text{kg}$ to final product value of $0.0750 \text{ MPa}\cdot\text{m}^3/\text{kg}$. An increase in ultimate strength and young's modulus also occurred. Ultimate strength increased 1.75 times from 7.849MPa to 14.375MPa and Young's modulus almost doubled at 1.8 times increase from 156.66MPa to 284.12MPa respectively.

INDEX WORDS: Thesis, Composite materials, Hierarchical, Cellulose, FormLabs, 3D printing, Georgia Southern University.

SYNTHESIS AND BEHAVIOR CHARACTERIZATION OF MULTI-SCALE
HIERARCHICAL STRUCTURED COMPOSITES

by

JACOB MAYFIELD

B.S., Georgia Southern University, 2015

A Thesis Submitted to the Graduate Faculty of Georgia Southern University in

Partial Fulfillment of the Requirements for the Degree

MASTER OF SCIENCE

STATESBORO, GEORGIA

© 2018

JACOB MAYFIELD

All Rights Reserved

SYNTHESIS AND BEHAVIOR CHARACTERIZATION OF MULTI-SCALE
HIERARCHICAL STRUCTURED COMPOSITES

by

JACOB MAYFIELD

Major Professor: Shaowen Xu
Committee: Aniruddha Mitra
Haijun Gong

Electronic Version Approved:

May 2018

DEDICATION

This thesis is dedicated to my Father and Grandfather for always pushing me to do my best and never give up on my goals.

ACKNOWLEDGMENTS

I would like to thank Dr. Xu for giving me priceless skills and knowledge in the materials science section of engineering. I would also like to thank Luke Fussel, Talia Zamora, for supporting me through this thesis process. I also want to thank Emily Cunningham and Thomas Phelps for pushing me to complete this research.

TABLE OF CONTENTS

ACKNOWLEDGMENTS	3
LIST OF TABLES	6
LIST OF FIGURES	7
CHAPTER 1: INTRODUCTION	9
1.1 Background:	9
1.2 Motivation:	9
1.3 Objectives:.....	9
CHAPTER 2: LITERATURE REVIEW	11
2.1 Overview:	11
2.2 3D Printing:.....	11
2.3 Hierarchical Structure Fabrication:	12
2.4 Natural Composites:	12
2.6 Buckling:	14
CHAPTER 3: EXPERIMENTAL METHODOLOGY	16
3.1 Method Overview:.....	16
3.2 3D Structure:	16
3.3 Testing Design:	19
3.4 Initial Process:	21
3.5 Sample Placement:	21
3.6 IPA Exposure:	22
3.7 New Chamber:.....	23
3.8 Set Time:	23
3.9 Cellulose:.....	23
3.10 Corrected Method:.....	25
CHAPTER 4: FINDINGS AND ANALYSIS	28
4.1 Experimental Calculations:	28
4.2 Data:	29
4.4 Statistical Analysis:	57
4.5 Discussion:	63
Chapter 5: CONCLUSIONS.....	68

5.1 Conclusions: 68

5.2 Recommendations: 68

References 70

LIST OF TABLES

Table 1: Solid V2 Dimensional data.....	29
Table 2: Initial method dimensions.....	30
Table 3: Sample Placement Dimensions.....	32
Table 4: IPA wash times dimensions.....	33
Table 5: Qualitative time data.....	34
Table 6: Old vs. New method dimensions.....	35
Table 7: Set time method dimensions.....	36
Table 8: Optimized method dimensions.....	37
Table 9: Process compare dimensions.....	39
Table 10: Cellulose Dimensions.....	40
Table 11: Tough V2 vs. Cellulose Addition dimensions.....	49
Table 12: Material comparison dimensions.....	52
Table 13: Sample Results.....	54
Table 14: Ultimate Strength Statistical Analysis.....	58
Table 15: Young's Modulus Statistical Analysis.....	58
Table 16: Specific Strength Statistical Analysis.....	58

LIST OF FIGURES

Figure 1: (a-d) Bamboo structure. (Zhang, Wang, Keer, 2015)	13
Figure 2: Specimens (Obataya, Kitin, Yamauchi, 2007).....	14
Figure 3: Diamond Unit Cell.	17
Figure 4: Periodic Appearing Unit cells.	17
Figure 5: Final 3D model.....	18
Figure 6: Form 2 3D printer. (Formlabs, 2018.).....	19
Figure 7: Micro ADMET apparatus.....	20
Figure 8: Macro ADMET apparatus.	20
Figure 9: Sample placement in curing chamber.	22
Figure 10: Bar Cooling.	24
Figure 11: Pool Cooling.....	25
Figure 12: UV curing Vertical, flip 180°.....	26
Figure 13: UV Curing Horizontal, flip 90°.....	26
Figure 14: Solid V2 sample.	29
Figure 15: Solid V2 Stress vs. Strain.....	30
Figure 16: Pretest Stress vs. Strain.	31
Figure 17: Sample placement Stress vs. Strain.....	32
Figure 18: IPA 5-minute vs. 10-minute Stress vs. Strain.	33
Figure 19: Old vs. New chamber Stress vs. Strain.	35
Figure 20: Sample set time Stress vs. Strain.....	36
Figure 21: Tough V2 3D printed structure.	37
Figure 22: Stress vs. Strain (Tough V2 Structure).....	38
Figure 23: Process compare.....	39
Figure 24: Cellulose Bar cooled structure.	40
Figure 25: Bar vs. Pool cooled cellulose.	41
Figure 26: Pool cooled x20 (cross section).....	42
Figure 27: Pool cooled x100 (cross section).....	42
Figure 28: Pool cooled x30 (axial).....	43
Figure 29: Pool cooled x100 (axial).....	43
Figure 30: Bar cooled x20 (cross section).	44
Figure 31: Bar cooled x100 (cross section).	45
Figure 32: Bar cooled x30 (axial).	45
Figure 33: Bar cooled x100 (axial).	46
Figure 34: Cellulose x200 (SEM).....	47
Figure 35: Cellulose x400 (SEM).....	47
Figure 36: Cellulose x2000 (SEM).....	48
Figure 37: Final product with 3D structure and cellulose addition.	49
Figure 38: Tough V2 control vs. Multi-scale Cellulose Addition.	50
Figure 39: Tough V2(left) vs. Final Product(right).	51
Figure 40: Cellulose(left) vs. Final Product(right).	51
Figure 41: Material comparison Stress vs. Strain.	53

Figure 42: Ultimate Strength Bar Graph.....	55
Figure 43: Young's Modulus Bar Graph.....	56
Figure 44: Specific Strength Bar Graph.....	57
Figure 45: Ultimate Strength Materials Avg.	59
Figure 46: Young's Modulus Materials Avg.....	60
Figure 47: Specific Strength Materials Avg.	60
Figure 48: Optimized Avg.	61
Figure 49: Control Avg.	62
Figure 50: Final Product Avg.	63

CHAPTER 1: INTRODUCTION

1.1 Background:

Composite materials offer greater strength while reducing the required weight, this is an increase in specific strength. Natural materials balance these two results well as they have multiple scale structures. Natural science is important to several engineering disciplines. Using biological processes and structures, and applying them to engineering principles we can further understand how nature constructs. This designing concept is most commonly known as biomimicry. This research could give a better understanding to that of natural composite materials, composition and material properties behavior. This in return would help scientist not only better utilize, but assist in the intelligent design of composite materials. This research will also help others with the understanding of hierarchical structure design. Hierarchical materials are structures that have structures within themselves, the material can be defined as multi-scale. Multi-scale as in levels of recognized structures in the material from Macro, Micro, to Nano. When designing composite materials, it is important to create repeatable consistent material properties and this can be difficult without proper studying of the processing of these materials.

1.2 Motivation:

The majority of composite materials do not apply factors from nature in them such as multi-scale structures. Most manmade materials are homogeneous while natural materials are heterogeneous with multiple scales ranging from Macro to Nano sizes. The construction of composite materials on a multiple scale has not been studied to a high degree.

1.3 Objectives:

The objective of this research is to: (1) Determine if a composite structure will exhibit an overall increase in strength with a decrease in weight, if designed using hierarchical bio-mimicry.

(2) Experimentally investigate the specific strength performance of a hierarchical constructed composite.

CHAPTER 2: LITERATURE REVIEW

2.1 Overview:

This literature review contains relevant background information of the following topics; 3D printing, hierarchical structure fabrication, and buckling.

2.2 3D Printing:

Additive manufacturing (AM) is the process of creating 3D structured objects by adding materials in a layer-by-layer technique. Common technologies make use of a computer aided design (CAD) 3D modeling software, equipment with an extrusion method and layering material. Additive manufacturing's main use in industry thus far has been rapid prototyping to create a visual model, but not creating the actual part used in production. Most people believe Additive manufacturing methods like 3D printing with metals, resins, and plastics are fairly new technologies, but the processes have been around since the 1980's. In 1987 the stereolithographic 3D systems were invented, these systems use an ultraviolet (UV) light-sensitive polymer resin that is cured layer-by-layer by a UV laser (Wohlers et al 2014). This process is most commonly seen today in the FormLab's 3D printing machines. There are many other methods of 3D printing. The most common one people think of is the fused deposition modeling (FDM), where a plastic is heat extruded from a tip onto a heated base. Some other methods are, multi-jet modeling (MJM) which is much like printing on paper, and 3D printing (3DP) where the model is built in a container with a power substance. The availability of these techniques has created a revolution in the manufacturing industry, creating several companies and hundreds of universities that use some type of 3D printing in their production process. However, with that said, most are still only using it for rapid prototyping.

2.3 Hierarchical Structure Fabrication:

Natural materials in hierarchical multi-scale structures such as bamboo, bone, nacre, and lobster cuticle exhibit unique and excellent material properties. In nature, most structures formed in a multi-scale fashion are light in weight but have a high strength and toughness. This makes the research conducted in this paper extremely important to the advancement of composite materials. How to mimic and utilize these structures remains a great research challenge. The paper by Jingsong Peng, and Qunfeng Cheng, discusses the challenges and methods of successfully creating these hierarchical structures. The main part of the paper that influenced this research was the ice-templating technique which is “When the inorganic ceramic slurry is frozen, the growing ice crystals entrap ceramic particles to be repelled from the interface, generating a laminate architecture.” (Peng, Cheng, 2017). Essentially, ice-casting is the method of freezing a slurry-like material in such as fashion to control how the ice forces the laminate structure to be cured in a repeatable way. The creators of this process had much success creating a composite structure that directly mimicked the organic structure under study and saw that the components in this arrangement could promote higher toughness and increase strength. The paper also goes into details about combining 3D printing and several other methods it lists the successes other researchers have had these methods or creation.

2.4 Natural Composites:

Bamboo consists of hierarchical structures on multiple length scales. The culm, more commonly known as the stem, has periodically appearing nodal structures along the longitudinal axis. The stem with the nodal structures can be seen in figure 1(a). It consists of parallel macro fibers that span the length between the nodal structures. The macro fibers actually tangle together to create these nodes. The macro fibers consist of hundreds of microfibers, which are functionally graded and distributed along the radius of the bamboo shown in figure 1(b) with a closer look at

individual fibers in figure 1(c). These microfibrils are constructed of multiple concentric co-shell structures that can be seen in figure 1(d).

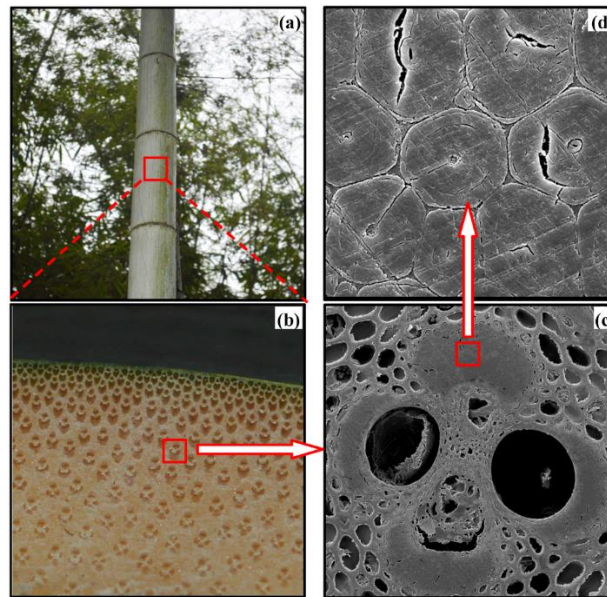


Figure 1: (a-d) Bamboo structure. (Zhang, Wang, Keer, 2015)

Bamboo is an important natural material all throughout Asia. Bamboo has large flexural deformation because, its outer fibrous layer can retain high tensile stress, and the inner porous foam like layer can withstand large compressive deformation (Obataya, Kitin, Yamauchi, 2007). Many studies have been performed on the mechanical structural and properties of bamboo. With bamboo exhibiting more of a ductile material comparatively to other wood. Obataya, Kitin, and Yamauchi, mention that bamboo should be studied more for not only its utilization, but also for intelligent material designing. They created and tested their samples for a four-point bend test. Their geometry for their samples can be seen below in figure 2.

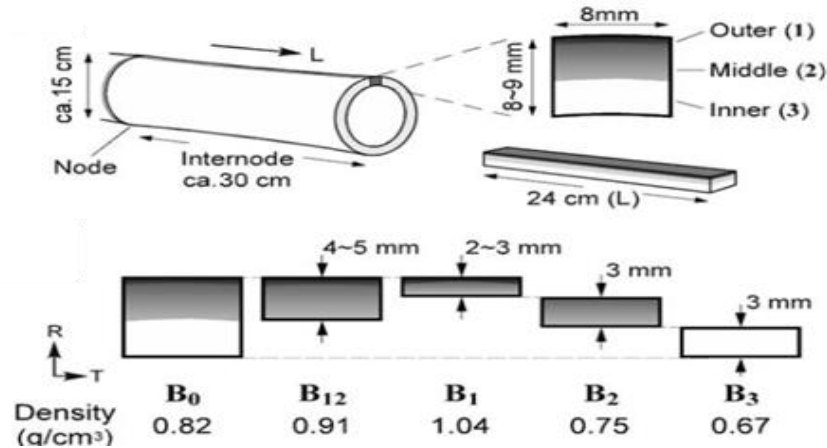


Figure 2: Specimens (Obataya, Kitin, Yamauchi, 2007).

2.6 Buckling:

The maximum axial load that a member can support when about to buckle is called the critical load. When a member is designed it is important to satisfy specific strength, deflection, and stability requirements. When large compressive loads are applied to some members, that are long and slender, the loading can be large enough to cause deflection in the lateral direction. These members are called columns when subjected to these types of forces, and the lateral deformation is called buckling. When the column is buckles, there is a small restoring force that is attempting to keep the column vertical. If this restoring force is greater than the compressive axis forces the column is in stable equilibrium and the column will remain vertically straight. If the compressive force is greater than the restoring force then the column becomes unstable and cannot support the load, causing the column to have a slight displacement. The final case is when the load is at critical load, and the column is in neutral equilibrium, where no slight force will not cause it to move further out of equilibrium, or be restored to its original position. Whether a column will remain stable or not when subjected to a compressive axial loading depends on the column's ability to restore itself, or simply put its resistance to bending (Hibbeler 2011). Critical stress in the column is an average normal stress, that is elastic stress, just before the column buckles, so the critical

buckling stress is less than or equal to that of the yield stress of that material. Another important part of buckling is the slenderness ratio, which is a measurement of the column's flexibility. The slenderness ratio is where the smallest radius of gyration of the cross section, the highest value of this ratio is where the buckling will take place.

CHAPTER 3: EXPERIMENTAL METHODOLOGY

3.1 Method Overview:

The methodology of this study is broken down into ten sections. These parts identify the changes to the processing of the samples to a quality analysis of each of the samples removing as many of the unwanted variables affecting the material properties as possible. The aforementioned sections are broken down in to two design sections of structure and Testing. Five sections of the 3D printed material Tough V2 optimization. Then one section for the Cellulose and a one final section for the corrected method of multi-scale material.

The first two design sections are the three-dimensional (3D) structure designed and printed using 3D printer, and the test design for the samples to accurately observe the materials properties. The initial process section where the processing of the 3D material was done to the Formlabs Inc. recommendations. The Sample Placement section refers to sample placement in the curing chamber. The New Chamber section shows the changing of the ultraviolet light(UV) curing chamber. The IPA Exposure section discusses the isopropyl alcohol(IPA) exposure time. The Set Time will show the effects of the set time of the samples after UV curing. Then the Cellulose section displays the comparison between two different cooling methods. Finally, the last section is the Corrected Method used in the final sample preparations.

3.2 3D Structure:

The structure created was a lattice structure of a periodic appearing diamond unit cell. The unit cell of diamond can be seen below in Figure 3. This unit cell is designed with four 0.4mm bars 1mm long from a central node all 120° apart from each other. Biomimicry was used by directly copying the naturally designed diamond unit cell.

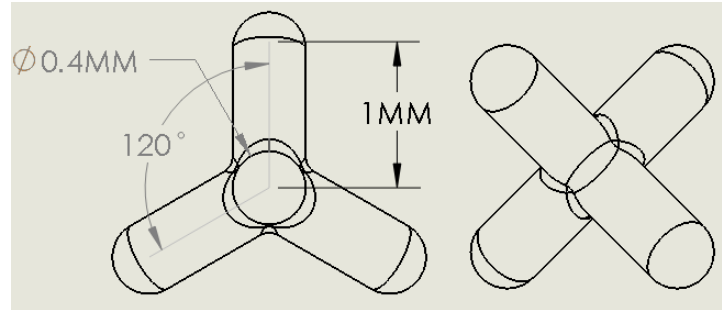


Figure 3: Diamond Unit Cell.

In Figure 4 one can notice the periodic appearing unit cells that form to make the following Figure 5 cylindric structure.

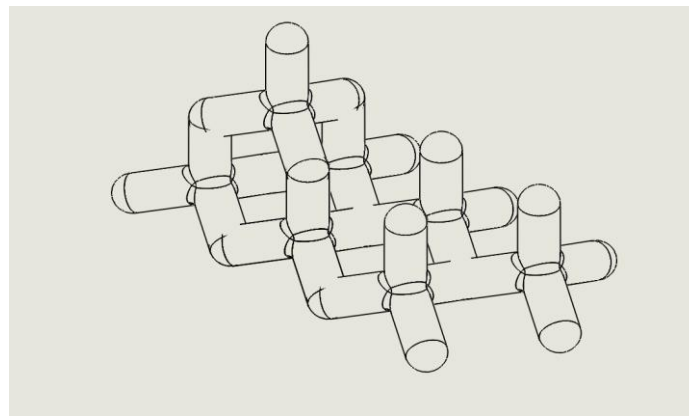


Figure 4: Periodic Appearing Unit cells.

The unit cell structure was then cut into a cylindrical shape of 19mm diameter and 50mm height which can be seen below in Figure 5. These dimensions were chosen so that the failure of the sample was predictable and would give an overall uniform stress across the structure.

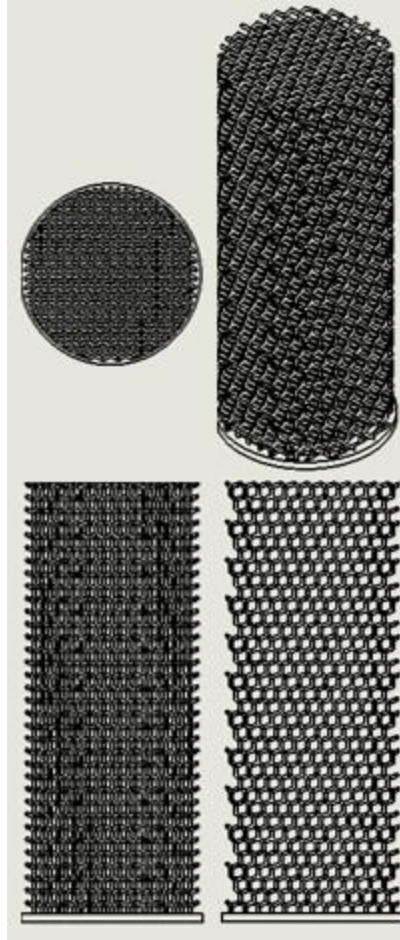


Figure 5: Final 3D model.

After this structure was created using Solidworks 2017-2018, the file was converted to an stl to be used to print on the Formlabs Form 2 printer a stereolithography(SLA) style 3D printer which can be seen below in Figure 6. The 3D printed material was a resin named Tough V2.



Figure 6: Form 2 3D printer. (Formlabs, 2018.)

3.3 Testing Design:

The samples were designed and printed for compressing testing. The testing apparatus used was an ADMET MTestQuattro. Two versions of this apparatus were used, one for micro testing and one for macro testing. The reason for this was the available load cells for each of the devices. The micro testing setup utilized a 444.8N (100 lb.) and a 2224.1N (500 lb.) load cell for the macro device. The 444.8N load cell was used for the preliminary testing due to the samples loads being low and unstable, once the sample processing was corrected the 2224.1N load cell was used. This load cell was an ADMET cell with an output of 1.41/1.852mV/V. This was connected to an ADMET controller that interpreted the voltage and set the information the testing software. The micro and macro setups can be seen below in Figure 7 and Figure 8 respectively. After the load cell was chosen the preload and feed rate of the test was determined. The preload was important to remove the slack from the tow of the graph to display a truer load and displacement curve. The preload was determined to be 2.5N while the feed rate was set to 5mm/min at 10 samples a second to achieve enough data points for a smooth line but not too many to introduce noise. The samples were compressed at until failure until the corrected method for processing the samples was achieved.

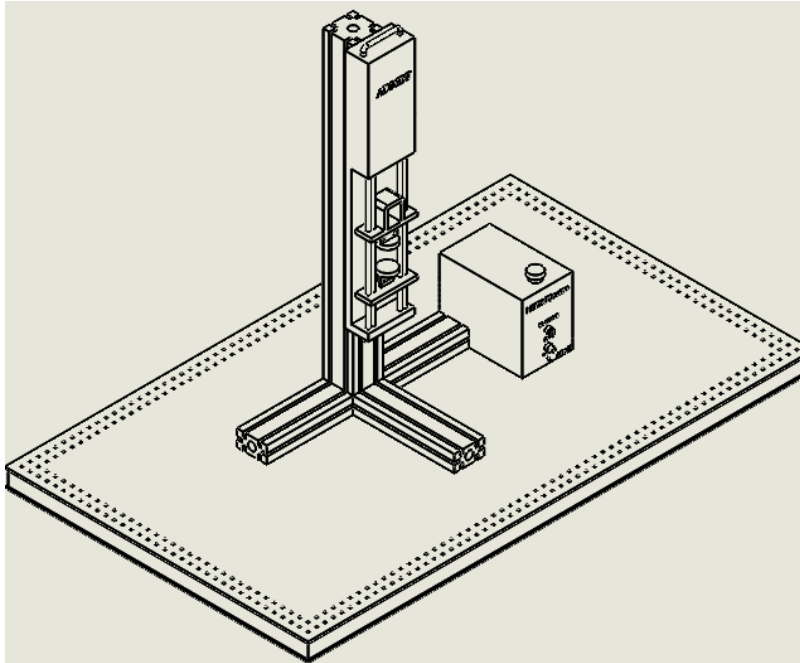


Figure 7: Micro ADMET apparatus.

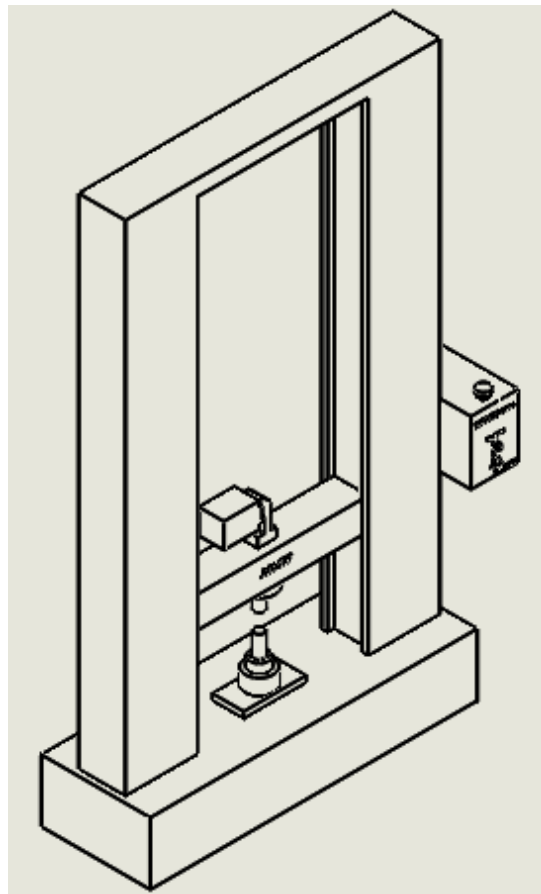


Figure 8: Macro ADMET apparatus.

3.4 Initial Process:

The initial chamber for curing the Formlabs Tough V2 material used in the 3D printed structure, is the suggested nail salon edge. It uses 365nm wavelength UV blubs to cure the samples. It is below the recommended 405nm wavelength source, but still provides a consistent chamber for curing for this research. The recommendation with this chamber is to use longer exposures or higher temperatures to achieve higher material properties such as strength. The research began by using the recommended times from Formlabs data sheet which was 60 minutes at 45°C. These times were then extended to test if the material properties could be increased. As the only negative effects of longer curing times are known to be shrinkage. The Formlabs process was a 2-minute shake, 10-minute Isopropyl alcohol bath, then another 2-minute shake, 10-minute IPA bath. After that the sample should be air dried and then cured using an ultraviolet light lamp, rotating sample for even curing as needed, then tested directly after. The curves produced by this method were highly sporadic with inconsistent values of ultimate stress, yielding points, and Young's modulus. So, it was necessary to start removing the variables from their process to better prepare more consistent samples.

3.5 Sample Placement:

The first variable for the samples was placement in the UV curing chamber. The placement method in the UV curing chamber. By recording the peak values and the sample location in the curing chamber, the correlation between weaker samples and their placement toward the front of the chamber was made. So, all the samples were then moved to the rear of the chamber to receive the same amount of UV light. This change in placement can be seen in Figure 9 below where sample. The sample near the back or rear of the chamber always was 20% higher yielding point so the conclusion was for all of the samples to be placed near the rear of the chamber

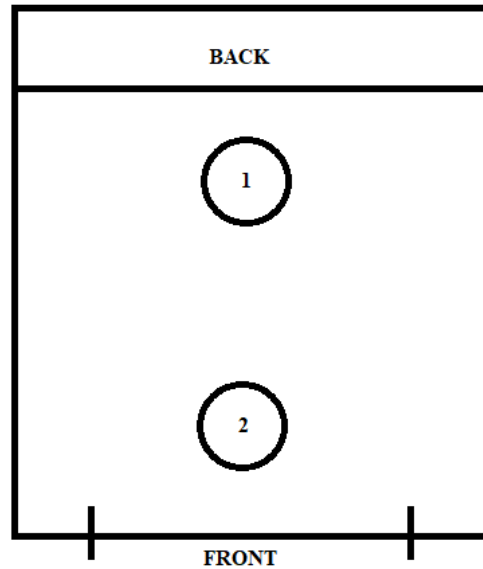


Figure 9: Sample placement in curing chamber.

3.6 IPA Exposure:

The samples for this methodology test were washed in IPA for varying time intervals to test for the wash procedure time. A comparison between 10-minute and 5-minute IPA wash time was done to try to achieve a more consistent grouping of stress vs. strain data. Also note for the IPA wash times the 405nm light chamber was used. It was clear that by halving the time down to 5-minute IPA bath the samples become a more consistent grouping until the yielding point of the material, using this information the choice to continually lower the IPA time was made. These time intervals to qualitatively test would start at 2 minutes to 30 seconds. Formlabs stated that the IPA bath should not affect the rigidity of the sample so each sample was compared to a control T_0 . All samples washed for longer than 30 seconds showed extreme flexibility and volume expansion not exhibited by T_0 . This qualitative test showed that the sample IPA bath time should be lower than 30 seconds.

3.7 New Chamber:

The curing chamber used first was a 365nm wavelength lamp. The decision to create a new chamber with the 405nm lamp was taken. New chamber was designed to meet the 405nm wavelength light. This chamber was used to cure several samples and still noticeable inconsistent material properties were present. The samples produced were noticeably lower overall yield points, ultimate strength, and Young's modulus. After verifying the sample placement and IPA time to the corrected amount some variation in the stiffness and consistency of yielding points still existed. This chamber was deemed to be unfit for the samples as comparable testing procedures produced overall lower peak load values and a less desirable curing time due to the intensity of the UV light emitted from the chamber. The stress value was used to determine this, the 405nm chamber produced much lower ranges of stress values than the 365nm. This was due to the intensity of the light produced by the UV LED's rather than the UV blubs in the old chamber. The old chamber with the 365nm wavelength light was chosen to be used during the research due to time constraints on perfecting a 405nm chamber.

3.8 Set Time:

The only remaining factor still existing that could possibly be affecting the variations in the samples could be the set time of the samples. This was testing using samples that set for 1 hour before testing and samples that set for 1 day before testing. It was extremely clear that the samples that were allowed to set longer were exposed to more moisture or deterioration of the IPA leading to a correlation between longer set time and lower more inconsistent data.

3.9 Cellulose:

After proper processing techniques were discovered for the formlabs tough V2 3D printed material the next step was to determine the best method for the addition of the cellulose to create a multi-scale material. The cellulose used in this research was a Cellulose Nanofibrils (CNF)

obtained from the university of Main process development center. This cellulose was 3% solid with a 90% fines rating. The nano-cellulose could be inserted into the micro-truss system to in theory help support the trusses much like rebar and concrete. There were two methods created for cooling the cellulose to an ideal shape. These two methods were Pool cooling and Bar cooling. Bar cooling can be seen below in Figure 10. Bar cooling is where the cellulose mold was set on top of an aluminum bar to cool the sample by ice casted forcing all the structure to cool from the bottom to the top creating long fibrous ice structures in the vertical direction. This method is similar to the method used by Munch et al. (Munch et al, 2008)

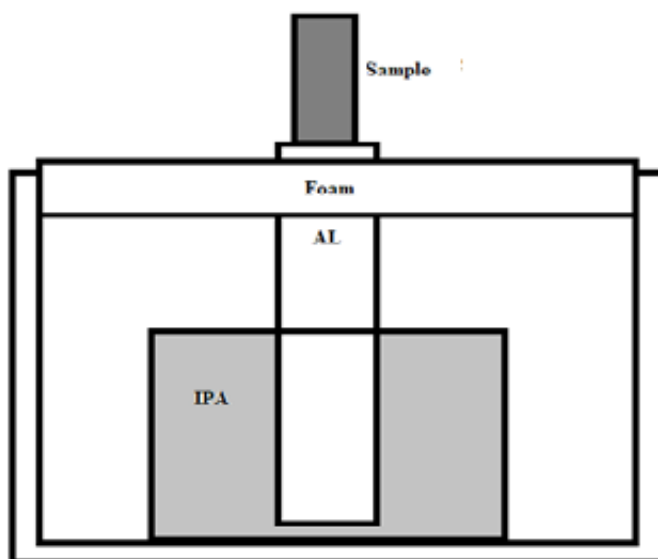


Figure 10: Bar Cooling.

Pool cooling can be seen below in Figure 11. Pool cooling is where the cellulose mold was set inside a container filled with IPA at -87°C in a Stirling Ultracold freezer and cooled uniformly from the outside in.

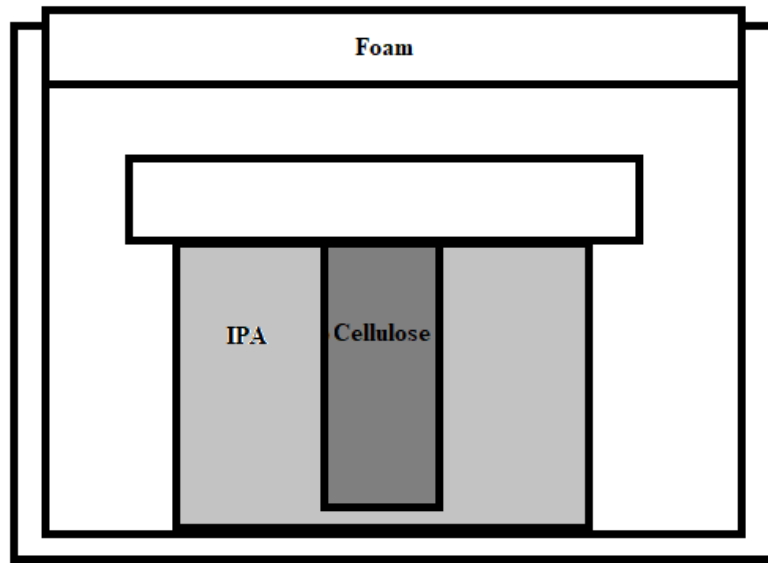


Figure 11: Pool Cooling.

Once reaching equilibrium for both methods, the samples were removed and immediately wrapped in a labeled paper towel and placed in a vacuum drier FreeZone at -56°C and 0.012mbar for three days to remove all moisture from the samples leaving just the structure formed by the cellulose freezing. The Pool cooling method provides a more uniform structure due to the ice formation in all directions from outside in. The Bar cooling method creates a better sample for compression and tension due to the long fibrous type ice formation in the vertical direction. These cellulose samples were then compression tested with a 0.25N preload and the same 10 samples a second at $5\text{mm}/\text{min}$ feed rate. Due to the overall stiffness and strength increase the Bar cooling method was chosen as the best method.

3.10 Corrected Method:

Once the appropriate method was decided, the following process was created. The samples were removed from the excess resin was removed with compressed air and then each sample was washed in Isopropyl alcohol (IPA) for 15 seconds then force dried using compressed air to remove

IPA from the samples surface. The samples were then allowed to set for two hours, and placed in the curing chamber of 365nm wavelength light at 50°C vertically for one hour as shown on Figure 12. When finished the samples were flipped 180° vertically and set for another hour. Next the sample were then flipped on its side and cured four times rolling the sample 90° every five minutes, shown in Figure 13. The samples were then allowed to set for one hour before testing. The diameter, length, and mass of each sample was taken at this time and recorded in a table. During testing the peak load value was recorded.

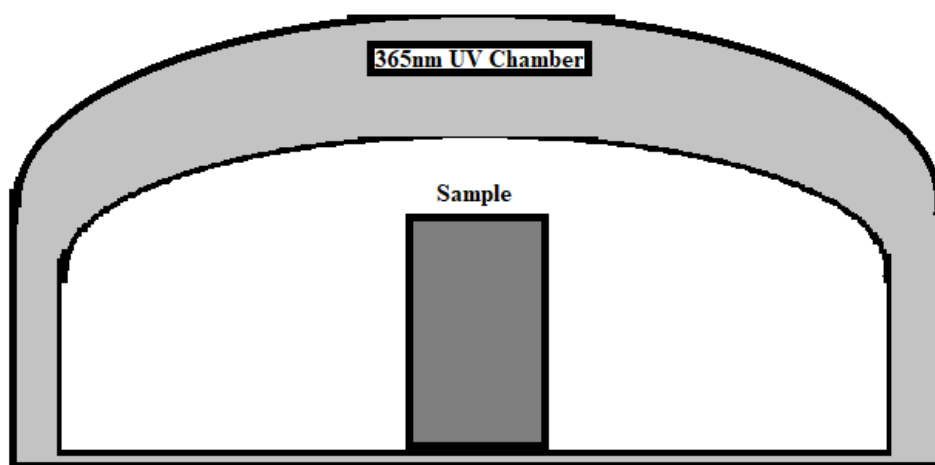


Figure 12: UV curing Vertical, flip 180°.

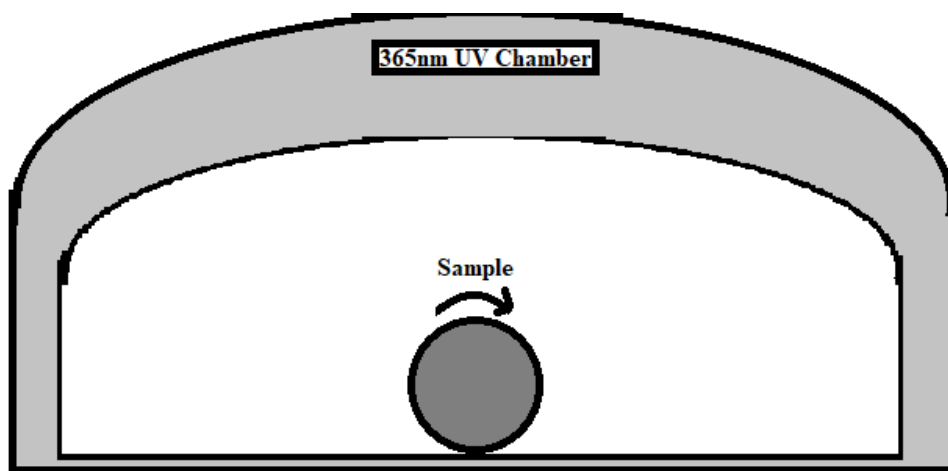


Figure 13: UV Curing Horizontal, flip 90°.

Once the methods were refined and selected the corrected method for the final product was tested. This involved the creation of the multi-scale material with Formlabs Tough V2 resin to be printed into a micro-truss system of diamond unit cells to be filled with cellulose and ice casted on a Stirling Ultracold freezer and dried in a FreeZone vacuum dryer. With consistency of the base Tough V2 material was achieved six samples were prepared these six samples had to be created using three different set of samples due to the ability to only print a specified max four samples at a time. Using the aforementioned methodology three of these samples were set aside as control samples for the Tough V2 since set time was a big correlation factor in the strength of the samples. The other three samples were then placed in a mold and filled with cellulose, these were then placed on top of an ice casting set up as shown in Figure 10 above, in a -86°C Stirling Ultracold freezer. These samples were ice casted for four hours to reach equilibrium temperature. Once reaching equilibrium they were removed and immediately wrapped in a labeled paper towel and placed in a vacuum drier FreeZone at -56°C and 0.012mbar for three days to remove all moisture from the samples leaving just the structure formed by the cellulose freezing. The samples that were ice casted were then tested at the same time as the control samples to ensure that the only variable was the addition of the cellulose to the 3D printed structure.

CHAPTER 4: FINDINGS AND ANALYSIS

4.1 Experimental Calculations:

Each test in this research produced load and displacement data, utilizing that and the dimensions of each sample the stress and strain values and curves could be obtained using the following Equation 1 and Equation 2. The stress and strain values are denoted σ and ε respectively. Where F is the applied load, A_0 is the calculated area, and L_0 is the length of the sample, showing that ΔL is the change in length of the sample.

$$\sigma = \frac{F}{A_0} \quad \text{Equation 1}$$

$$\varepsilon = \frac{\Delta L}{L_0} \quad \text{Equation 2}$$

Next the max values of the stress were determined and used for the ultimate stress values. The Young's Modulus, denoted by E was also determined using two methods, first by graphically measuring the slope of the stress vs. strain curves till the yield point, and secondly by Equation 3, by dividing the stress by the strain.

$$E = \frac{\sigma}{\varepsilon} \quad \text{Equation 3}$$

The important factor of this research is creating a light but strong structure and the value that determines this quantifiably is the specific strength of the material. It is determined by the stress divided by the density of the material denoted as ρ . This equation is shown below in Equation 4.

$$\text{Specific Strength} = \frac{\sigma}{\rho} \quad \text{Equation 4}$$

The Solid V2 tested used a true stress vs. true strain calculation these equations can be see below in Equation 5 and 6 respectively. Where σ_t represents true stress and ε_t represents true strain.

$$\sigma_t = \sigma(1 + \varepsilon) \quad \text{Equation 5}$$

$$\varepsilon_t = \ln(1 + \varepsilon) \quad \text{Equation 6}$$

4.2 Data:

The first test was to test a sample of pure solid V2 material, this material can be seen below in Figure 14. Table 1 below is the dimensional data for the sample of pure V2, where Figure 15 is the stress versus strain curve produced using the calculated values of true stress and true strain. This material was cured using FormLabs designed processing recommendations.



Figure 14: Solid V2 sample.

Table 1: Solid V2 Dimensional data

Sample	Height(m)	Diameter(m)	Mass (kg)
Solid V2	0.02440	0.01498	0.00483

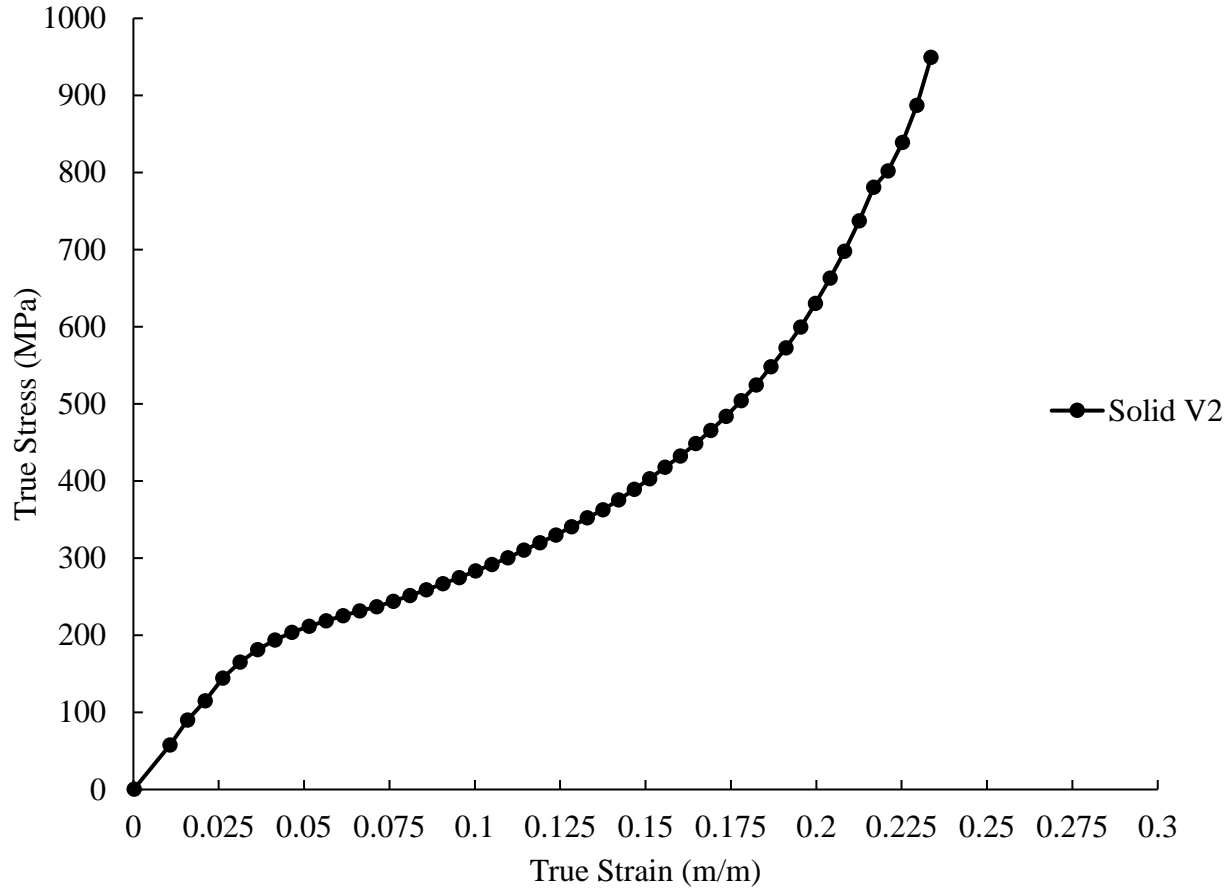


Figure 15: Solid V2 Stress vs. Strain

The first set of samples were tested using the initial method set by FormLabs. The following Table 2 is for the dimensions for this initial testing. The Figure 16 below displays the stress versus(vs.) strain curves for the initial testing.

Table 2: Initial method dimensions.

Sample	Height(m)	Diameter(m)	Mass (kg)
Pre1	0.04663	0.01890	0.00157
Pre2	0.04686	0.01887	0.00166
Pre3	0.04669	0.01880	0.00174
Pre4	0.04648	0.01871	0.00158

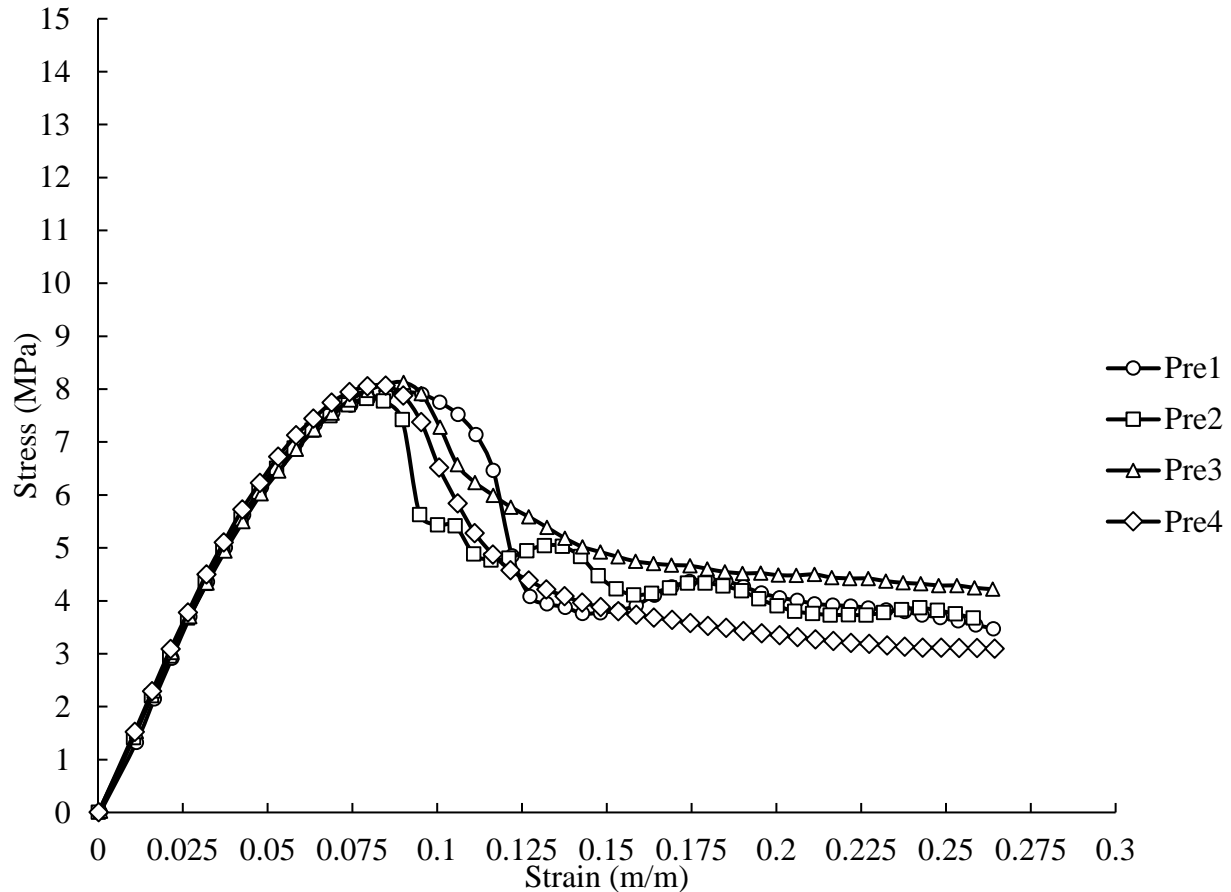


Figure 16: Pretest Stress vs. Strain.

The following data section was the first variable to be changed when attempting to optimize the processing of Tough V2 material. The samples for the placement were 1A1, 2B1, 1C2, and 2D2. Where the first number represents whether or not it was placed in the front or back of the chamber, the letter is the sample identifier, and the second number is the sample set. The dimensions for these samples can be seen below in Table 3 with the stress vs. strain curve in Figure 17 displaying the samples. One can notice the samples placed in the front of the chamber 2B1 and 2D2 were seeing less of the benefits from the UV light.

Table 3: Sample Placement Dimensions.

Sample	Height(m)	Diameter(m)	Mass (kg)
1A1	0.04673	0.01879	0.00173
2B1	0.04653	0.01879	0.00158
1C2	0.04666	0.01889	0.00173
2D2	0.04663	0.01889	0.00157

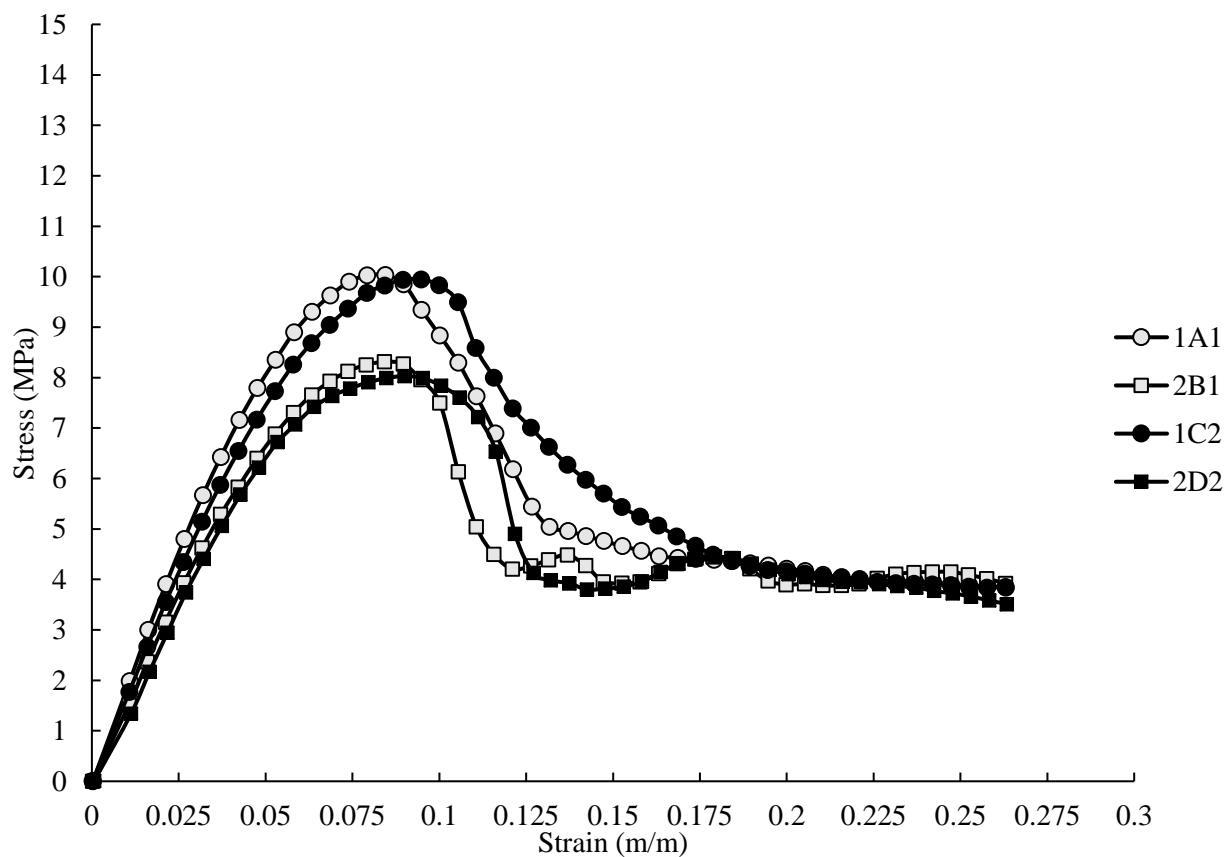


Figure 17: Sample placement Stress vs. Strain.

The data collected for the IPA wash duration was collected using the 405nm chamber, before it was deemed to produce undesirable results. The following Table 4 is the dimensions for the samples. 5A-5D and 10A-10D were subjected to 5 minute and 10 minute respectively. The stress vs. strain curves for these samples can be seen below in Figure 18, the more consistent clustering of the stiffness values can be seen directly.

Table 4: IPA wash times dimensions.

Sample	Time (min)	Height(m)	Diameter(m)	Mass (kg)
5A	5	0.04883	0.00995	0.00237
5B	5	0.04880	0.00979	0.00231
5C	5	0.04856	0.00993	0.00215
5D	5	0.04885	0.00987	0.00220
10A	10	0.04845	0.00989	0.00217
10B	10	0.04864	0.00987	0.00235
10C	10	0.04856	0.00984	0.00218
10D	10	0.04870	0.00984	0.00232

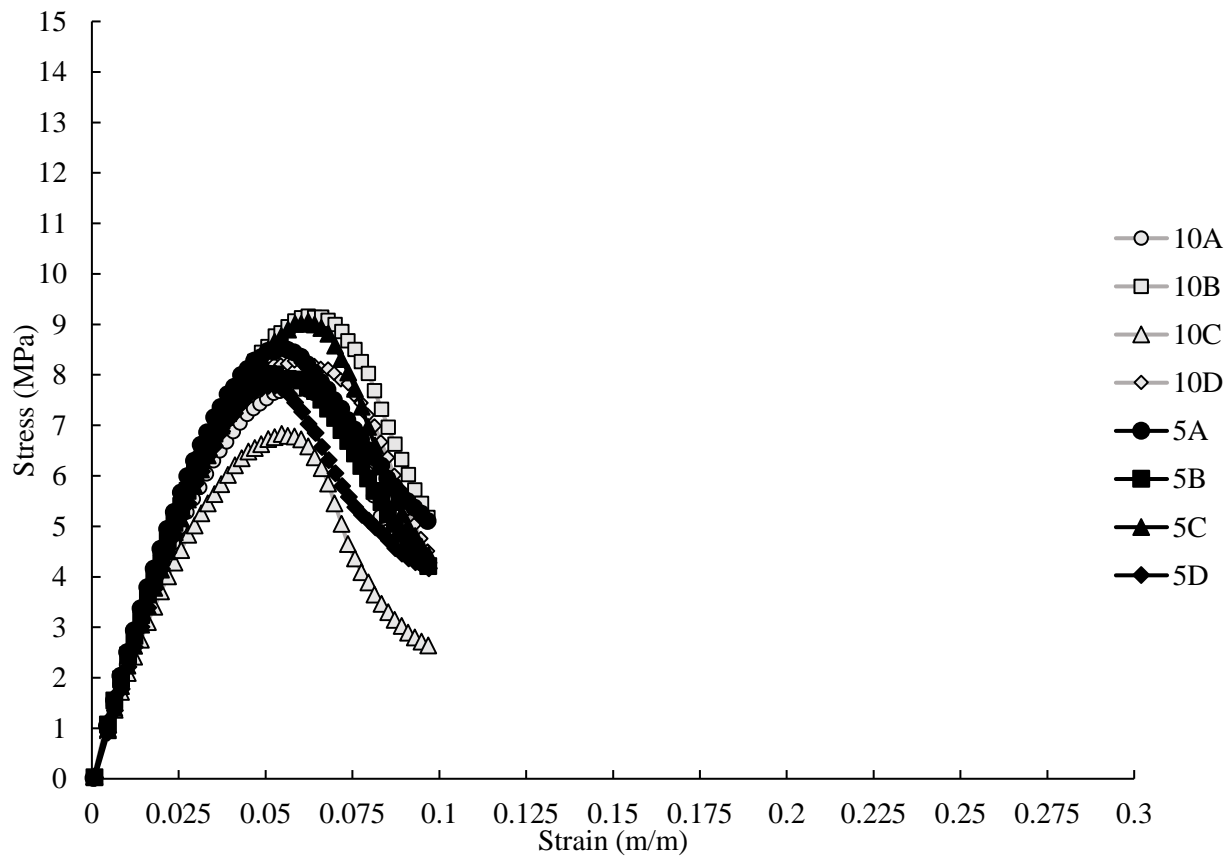


Figure 18: IPA 5-minute vs. 10-minute Stress vs. Strain.

The following Table 5 displays the qualitative results for testing the IPA wash time further.

The correlation for the lower wash time and the more consistent values gave attention that the IPA time needed further investigation to decide on the correct amount of IPA exposure. The time

intervals for qualitatively testing start at 120 seconds and halving the time until reaching the control time of T_0 since the control should have the same amount of rigidity and volumetric swelling as after being washed in the IPA.

Table 5: Qualitative time data.

Sample	Time (s) in IPA	Rigidity	Swelling
T_0	0	Good	none
T_1	30	Good	none
T_2	60	Flex	Small
T_3	120	High Flex	Large

After verifying the sample placement and IPA time to the corrected amount some variation in the stiffness and consistency of yielding points still existed and the consistency of the highest achieved values were not obtained. This chamber was deemed to be unfit for the samples as comparable testing procedures produced overall lower peak load values and a less desirable curing time due to the intensity of the UV light emitted from the chamber. The noting factor is the much lower range of stress values from 18 MPa average for the old chamber down to below 10 MPa for the new chamber. The old chamber with the 365nm wavelength light was chosen to be used during the research due to time constraints. The following Table 6 is the dimensions for the samples where the old and new chambers were directly tested against one another. The samples with labels New1-New2 are the new chamber or the 405nm wavelength. The samples with labels Old1 and Old2 are the old chamber or the 365nm wavelength. The samples stress vs. strain curves can be seen below in Figure 19.

Table 6: Old vs. New method dimensions.

Sample	Height(m)	Diameter(m)	Mass (kg)
Old1	0.04663	0.01890	0.00157
Old2	0.04686	0.01887	0.00166
New1	0.04851	0.01930	0.00208
New2	0.04869	0.01948	0.00197

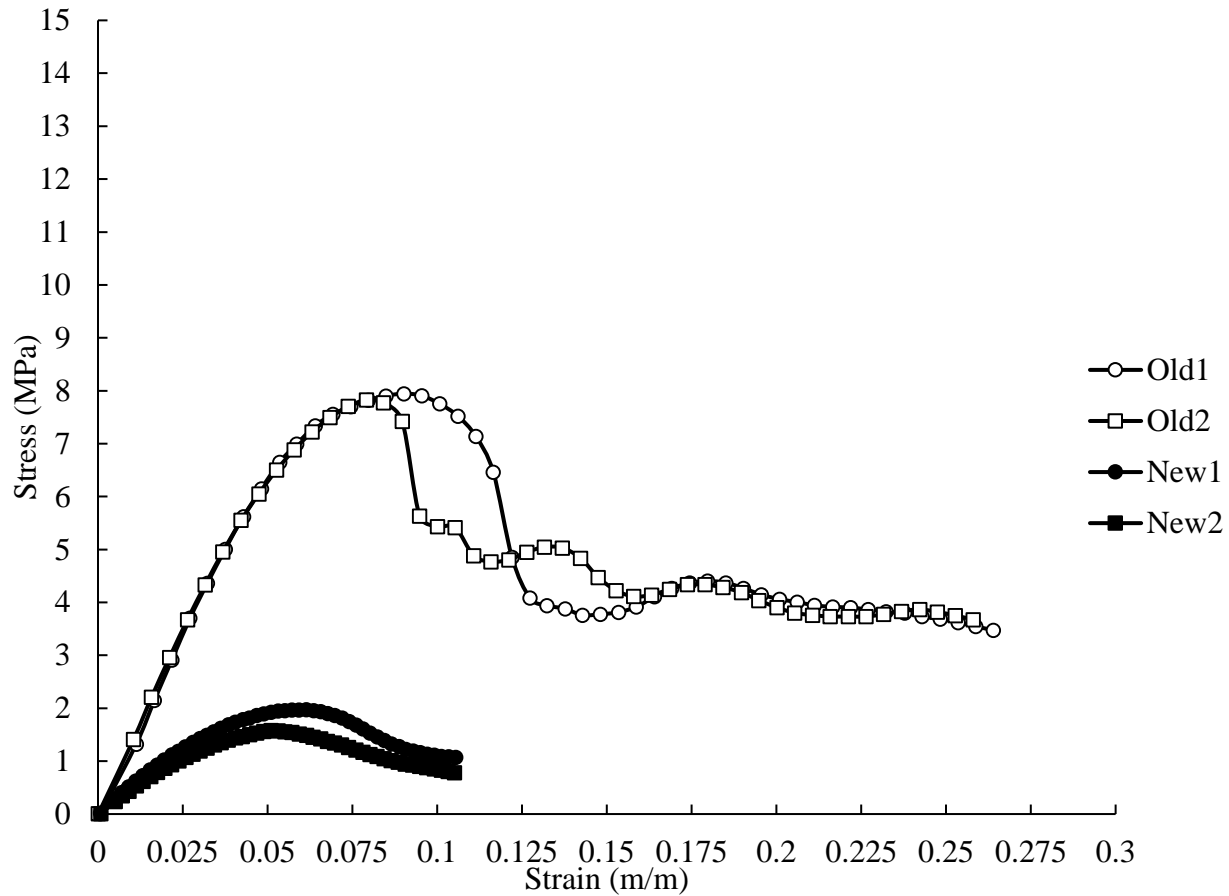


Figure 19: Old vs. New chamber Stress vs. Strain.

The next variable to test after removing the chamber UV light intensity issues was set time for the samples. The samples ST1 and ST2 were allowed to set for one full day after curing, and samples ST3 and ST4 only set for one hour before testing. The following Table 7 shows the dimensions and set times for these samples. The Figure 20 shows the comparison between the stress vs. strain curves for samples ST1-ST4.

Table 7: Set time method dimensions.

Sample	Height(m)	Diameter(m)	Mass (kg)
ST1	0.04938	0.02007	0.00220
ST2	0.04940	0.02007	0.00215
ST3	0.04930	0.01981	0.00237
ST4	0.04945	0.02004	0.00231

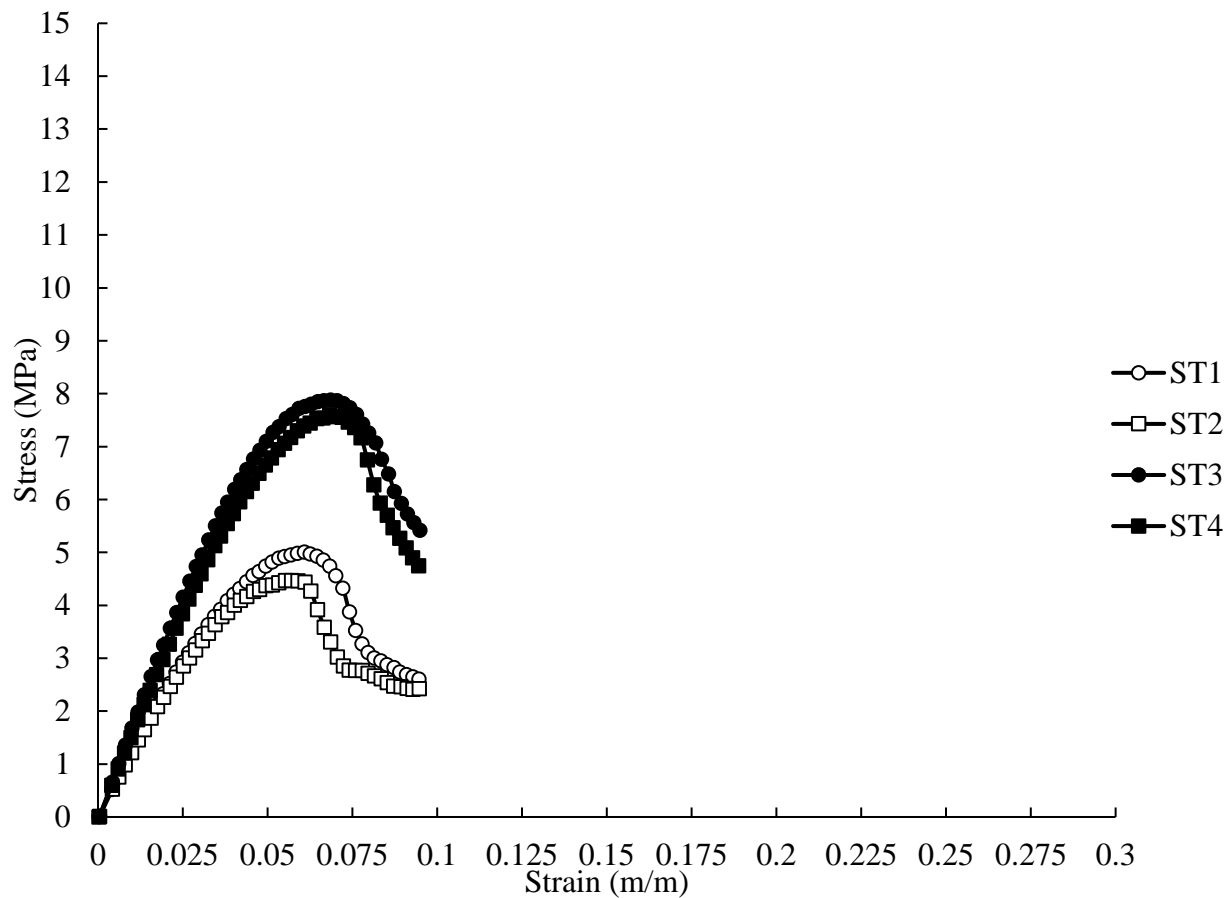


Figure 20: Sample set time Stress vs. Strain.

After all of the variables were removed the process was conducted using the new refined method which produced overall more optimal results. The dimensions for the more optimized

results can be seen below in Table 8. The stress vs. strain curves for the optimized method can be seen in Figure 22. The model printed can be seen below in

Figure 21.

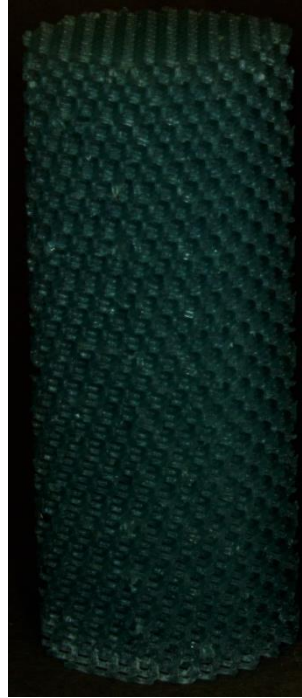


Figure 21: Tough V2 3D printed structure.

Table 8: Optimized method dimensions.

Sample	Height(m)	Diameter(m)	Mass (kg)
1	0.04998	0.02074	0.00310
2	0.04988	0.02080	0.00285
3	0.04990	0.02051	0.00291
4	0.04979	0.02051	0.00280

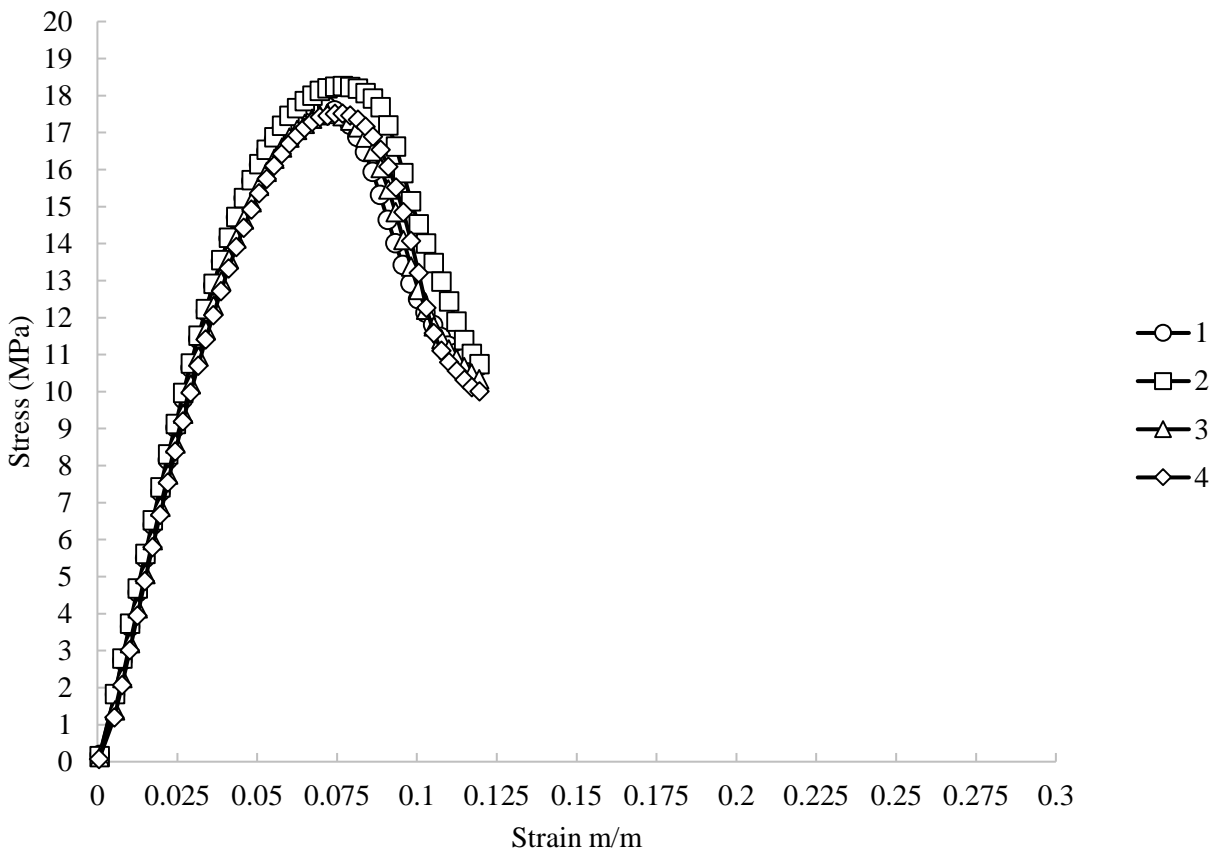


Figure 22: Stress vs. Strain (Tough V2 Structure).

The following Figure 23 is the comparison between the optimized method and the methods during the materials optimization process. Table 9 is the dimensions for the samples for comparison.

Table 9: Process compare dimensions.

Sample	Height(m)	Diameter(m)	Mass (kg)
Old1	0.04663	0.01889	0.00157
New1	0.04851	0.01930	0.00208
Pre3	0.04668	0.01879	0.00173
ST1	0.04938	0.02007	0.00220
ST3	0.04930	0.01981	0.00237
1	0.04998	0.02074	0.00310
5A	0.04883	0.00995	0.00237
10A	0.04845	0.00989	0.00217
1A1	0.04673	0.01879	0.00173
2D2	0.04663	0.01889	0.00157

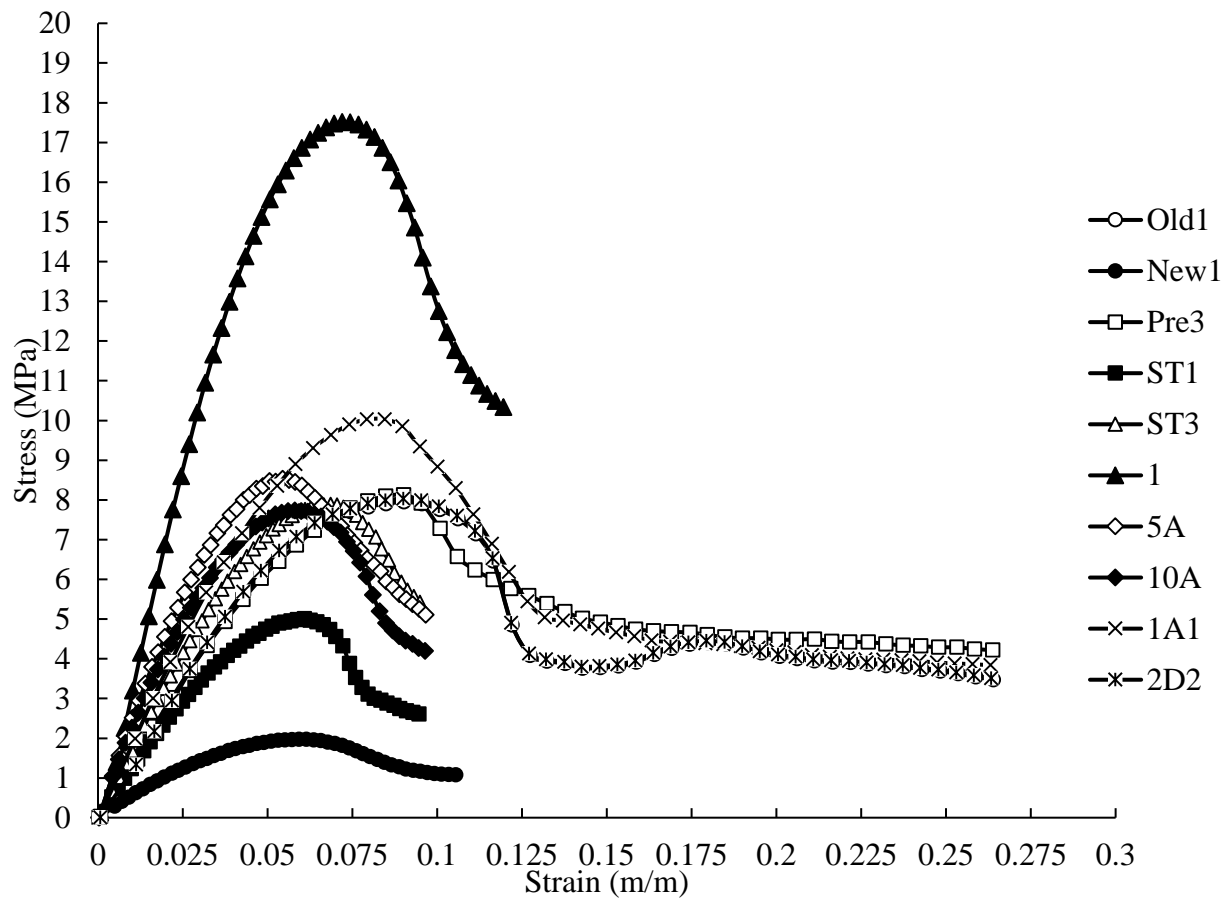


Figure 23: Process compare.

The cellulose cooling data was collected to determine the most optimized and efficient cooling method for the cellulose, to give greater strength to the overall finished product material. The two methods Bar and Pool cooling as discussed earlier produced unique results. The Table 10 below shows the samples dimensions after processing samples labeled PC1 and PC2 are Pool cooled and samples labeled BC1 and BC2 are Bar cooled. Their respective stress vs. strain curves can be seen below in Figure 25. The Bar cooled cellulose structure can be seen below

Figure 24.



Figure 24: Cellulose Bar cooled structure.

Table 10: Cellulose Dimensions.

Sample	Height(m)	Diameter(m)	Mass (kg)
BC1	0.05553	0.01826	0.00032
BC2	0.05539	0.01814	0.00032
PC1	0.04650	0.01859	0.00030
PC2	0.04678	0.01870	0.00029

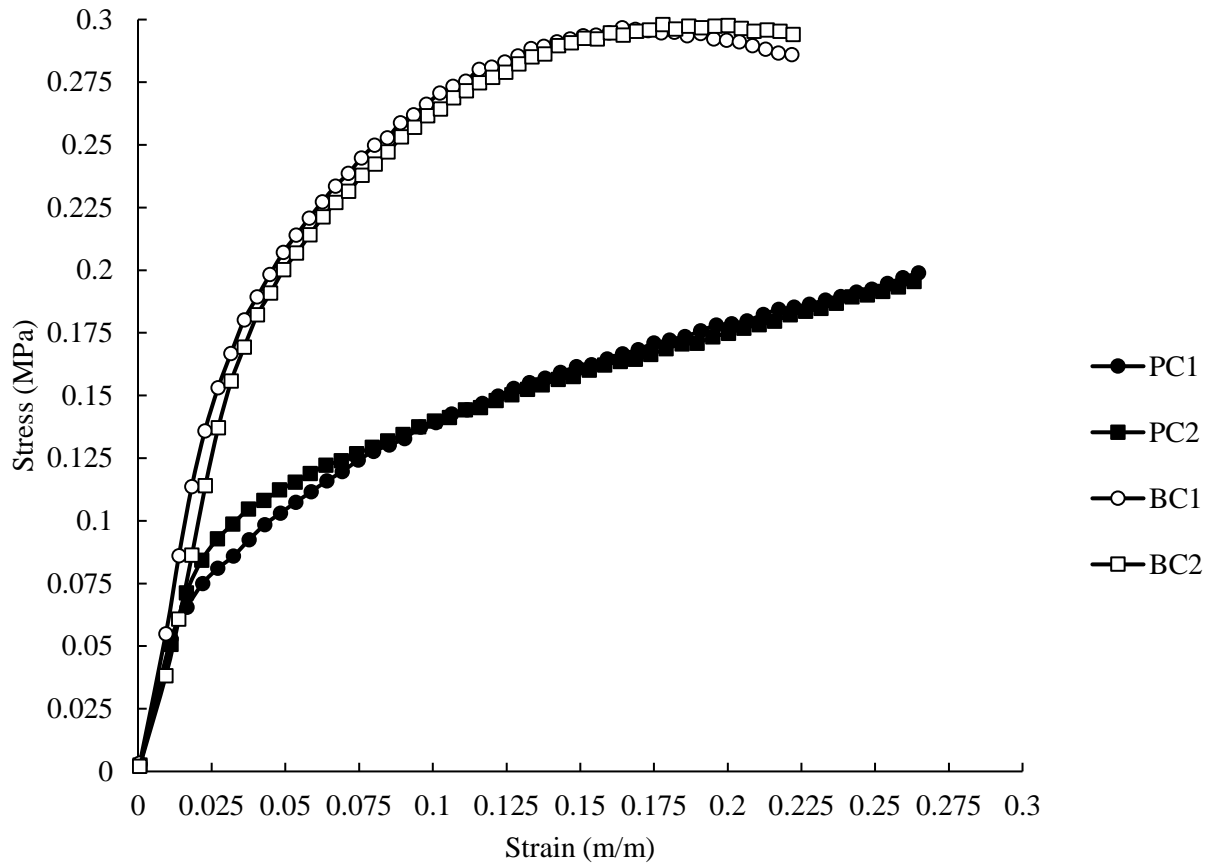


Figure 25: Bar vs. Pool cooled cellulose.

The cellulose was further investigated. The following figures below are the microstructure of samples BC1 and PC1 labeled appropriately. The figures are labeled accordingly to their magnification. The magnification of the samples was taken using the Keyence microscope. The following magnification and their respective figures for the cross section of the Pool cooled method are; x20 and x100, Figure 26 and Figure 27. The following magnification and their respective figures for the cross section of the Pool cooled in the axial direction are; x30 and x100, Figure 28 and Figure 29.



Figure 26: Pool cooled x20 (cross section).

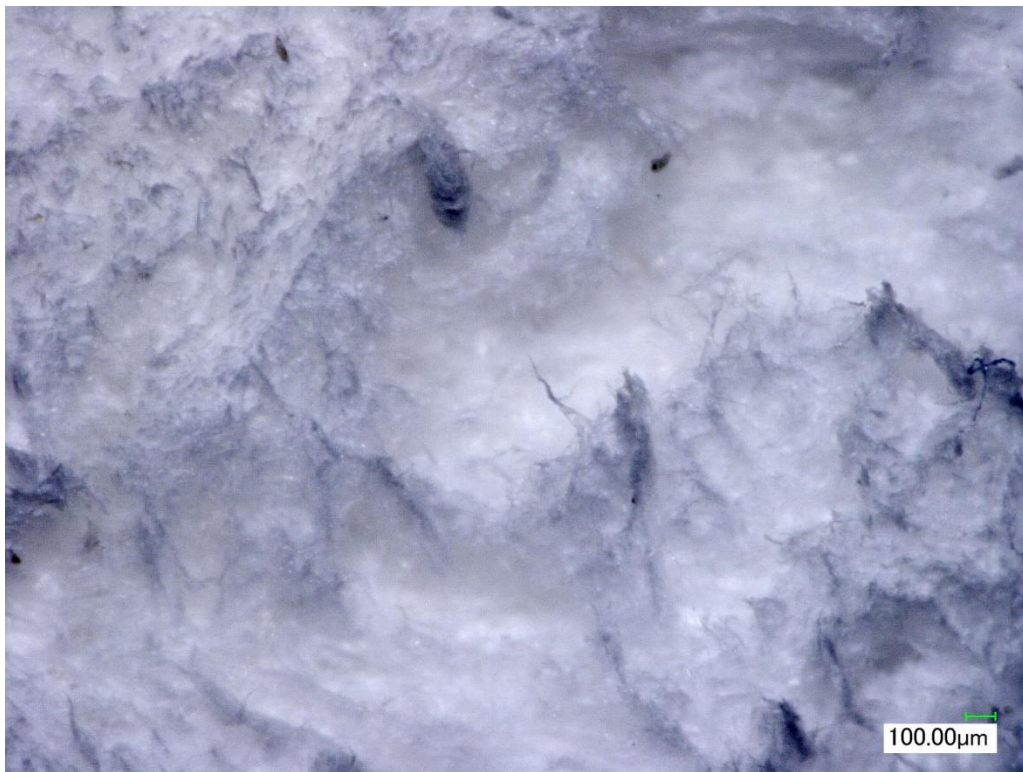


Figure 27: Pool cooled x100 (cross section).



Figure 28: Pool cooled x30 (axial).



Figure 29: Pool cooled x100 (axial).

The following magnification and their respective figures for the cross section of the Bar cooled method are; x20 and x100, Figure 30 and Figure 31 . The following magnification and their respective figures for the cross section of the Bar cooled in the axial direction are; x30 and x100, Figure 32 and Figure 33 .



Figure 30: Bar cooled x20 (cross section).

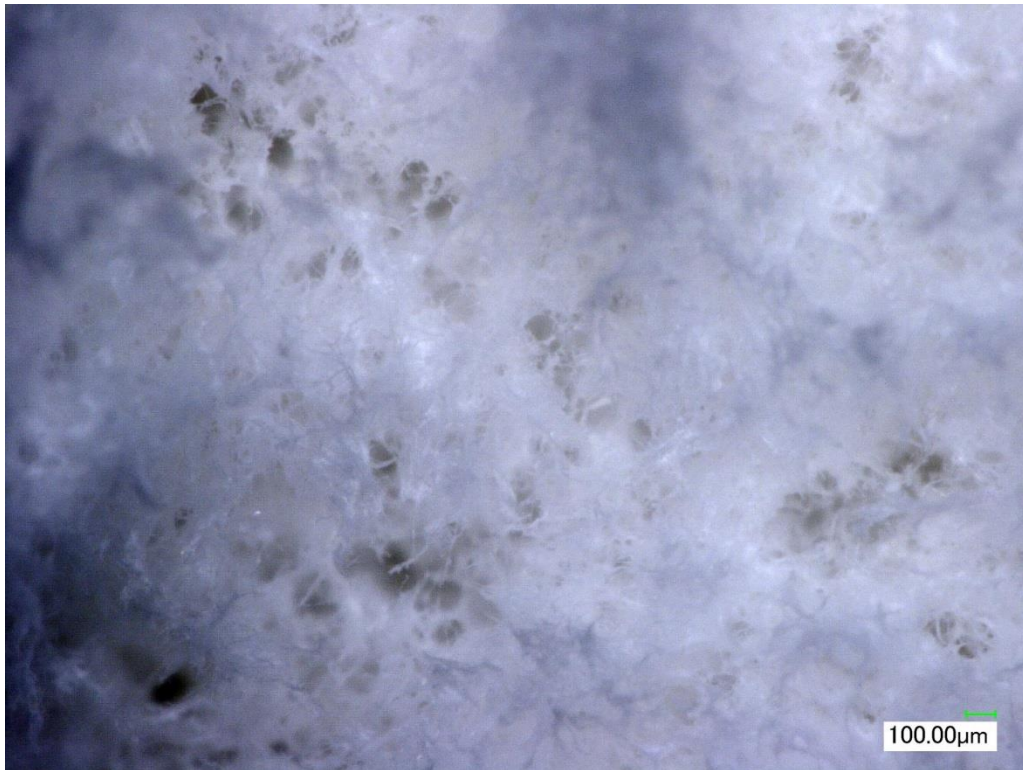


Figure 31: Bar cooled x100 (cross section).



Figure 32: Bar cooled x30 (axial).

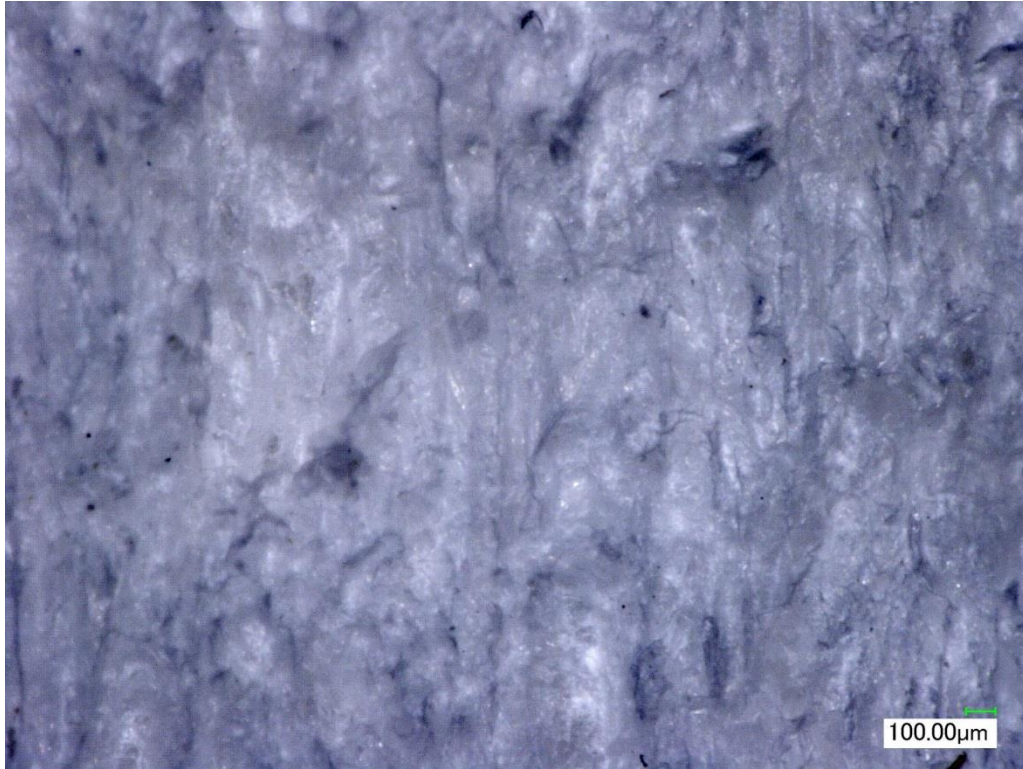


Figure 33: Bar cooled x100 (axial).

Figure 34, Figure 35, and Figure 36 were taken using an Electron Microscope (SEM) at magnifications of 200, 400, and 2000. After x200 magnification the differences between the PC and BC was indistinguishable, it is also important to note that the samples undergone a gold plating process.

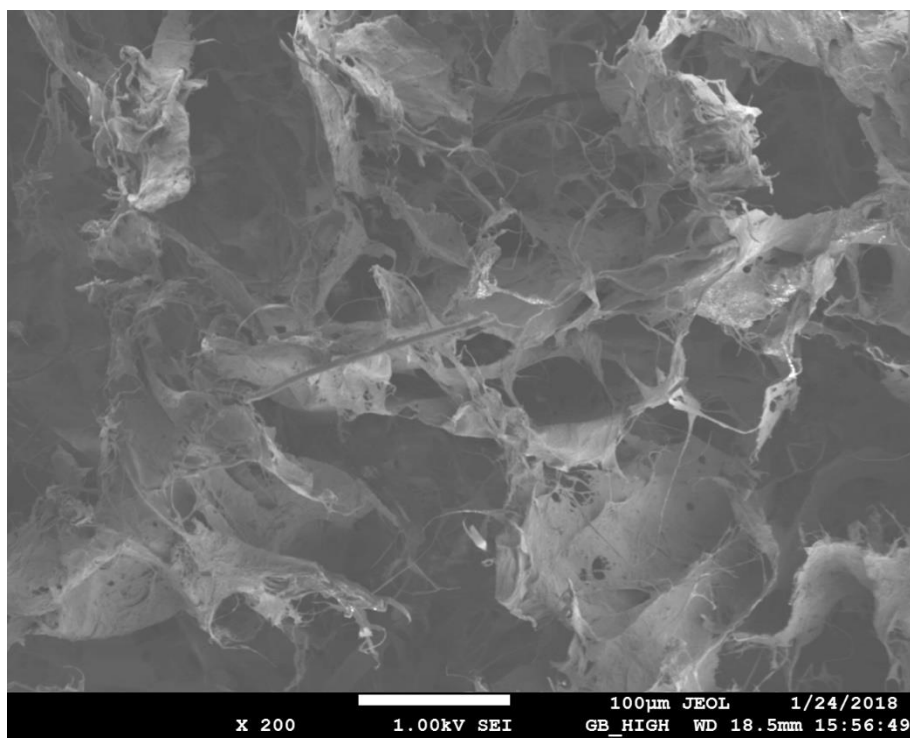


Figure 34: Cellulose x200 (SEM).

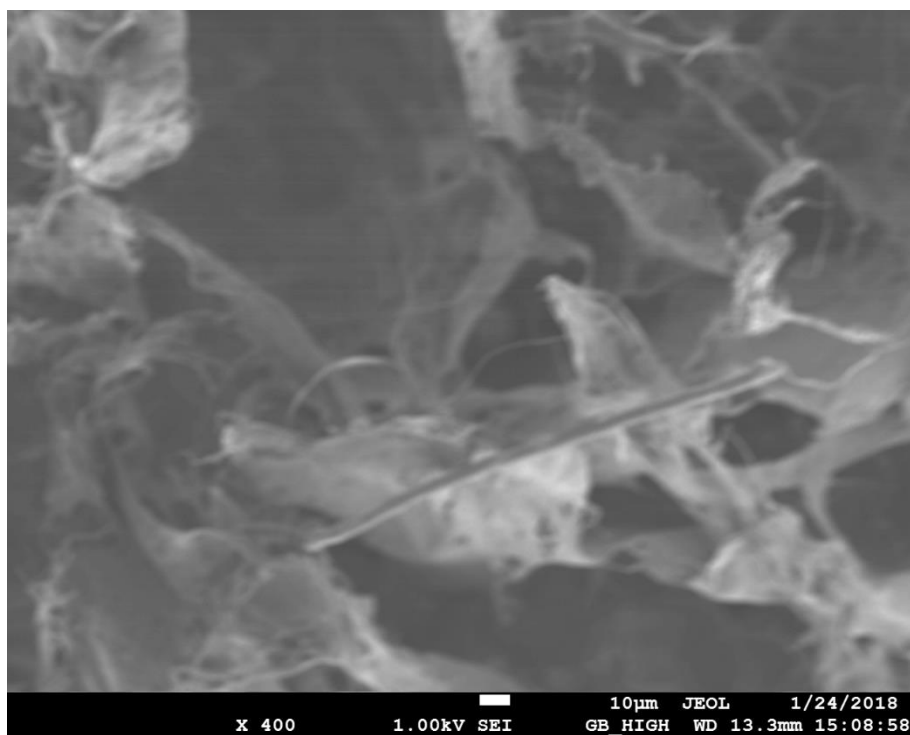


Figure 35: Cellulose x400 (SEM).

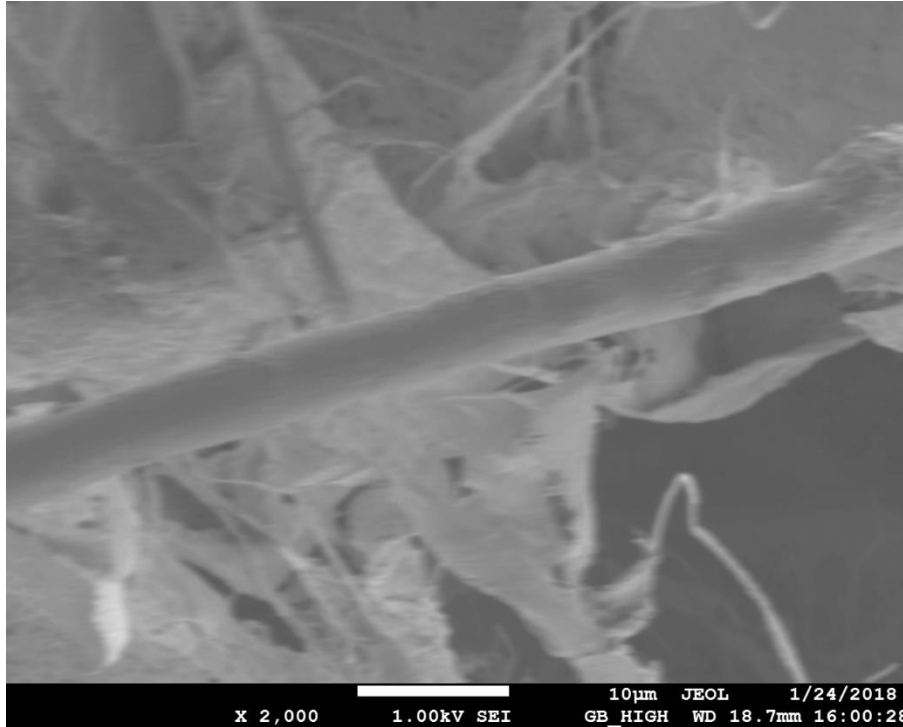


Figure 36: Cellulose x2000 (SEM).

Table 11 below shows the dimensions of the samples of the base materials (Tough V2) and the final multi-scale material, the base with the cellulose addition. The nomenclature for these samples is the letter B or C for the base or cellulose addition respectively. Then the first number 1 represents the set which it was removed from the printer, and the last number represents which sample it was. For example, B23 would be base material, set 2, sample 3. The stress vs. strain for these samples can be seen below in Figure 38. The final product can be seen in Figure 37 below.



Figure 37: Final product with 3D structure and cellulose addition.

Table 11: Tough V2 vs. Cellulose Addition dimensions.

Sample	Height(m)	Diameter(m)	Mass (kg)
B11	0.04981	0.02066	0.00278
B22	0.05004	0.02078	0.00297
B33	0.04972	0.02044	0.00287
C11	0.04979	0.01971	0.00292
C22	0.04961	0.01972	0.00287
C33	0.04986	0.01988	0.00288

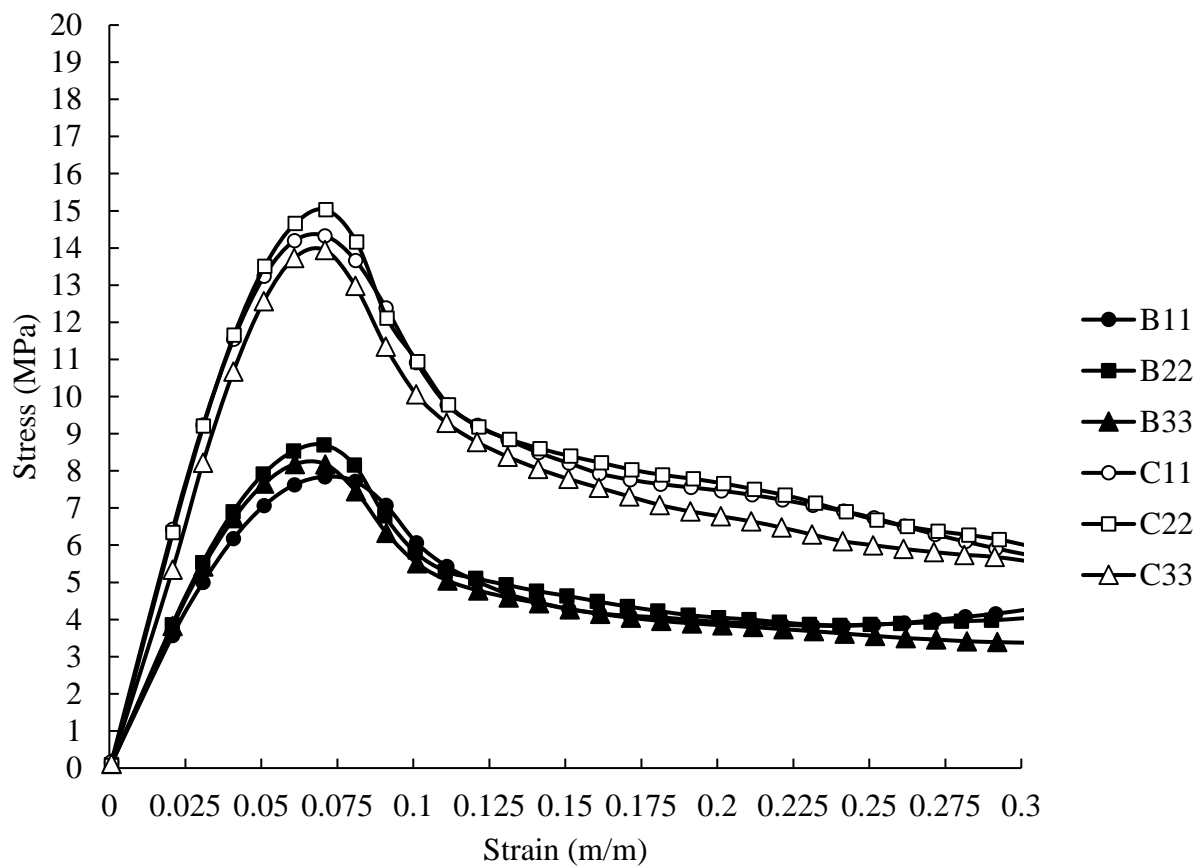


Figure 38: Tough V2 control vs. Multi-scale Cellulose Addition.

The comparison between the final product, the optimized control, and the Bar cooled cellulose, can be seen below Figure 39 in Figure 40 and respectively.

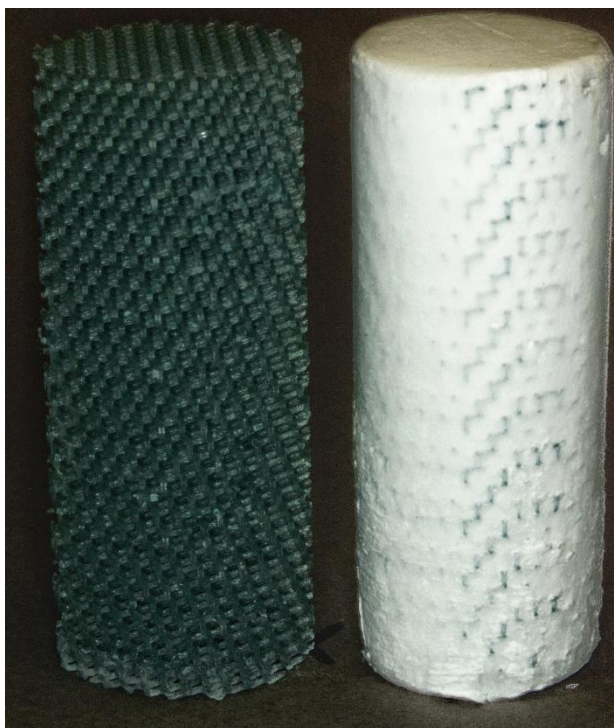


Figure 39: Tough V2(left) vs. Final Product(right).

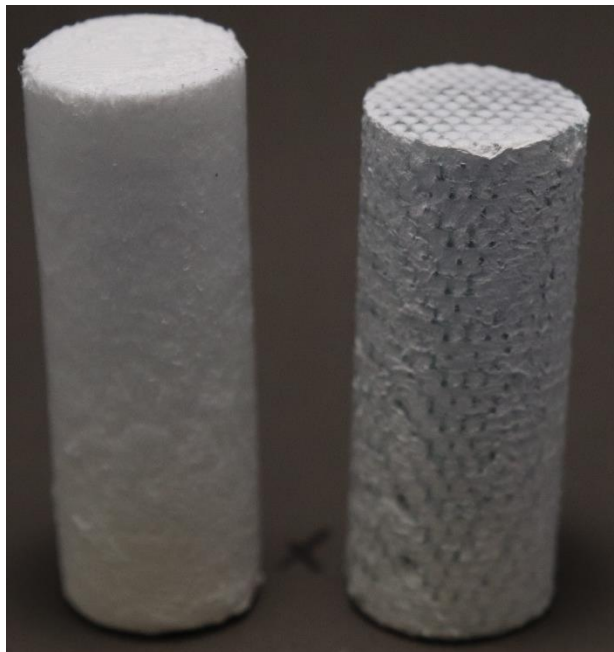


Figure 40: Cellulose(left) vs. Final Product(right).

The following Table 12 below is the dimensions for the comparison of the materials. The comparing materials are the Bar cooled cellulose BC1, the corrected method 1, the control B11, and the final product C11. These are also compared in Figure 41 using their stress vs. strain curves. The first noticeable element between the corrected method and the control were their difference in yield point values of the corrected method and the control. This is mainly due to the set time between the curing chamber and testing. The control set for 4 days due to the processing of the final product. Also, it is difficult to compare the cellulose values with the Tough V2 material due to the difference in values. Therefore, the specific strength is calculated and displayed below.

Table 12: Material comparison dimensions.

Sample	Height(m)	Diameter(m)	Mass (kg)
BC1	0.05553	0.01826	0.00032
1	0.04998	0.02074	0.00310
B11	0.04981	0.02066	0.00278
C11	0.04979	0.01971	0.00292

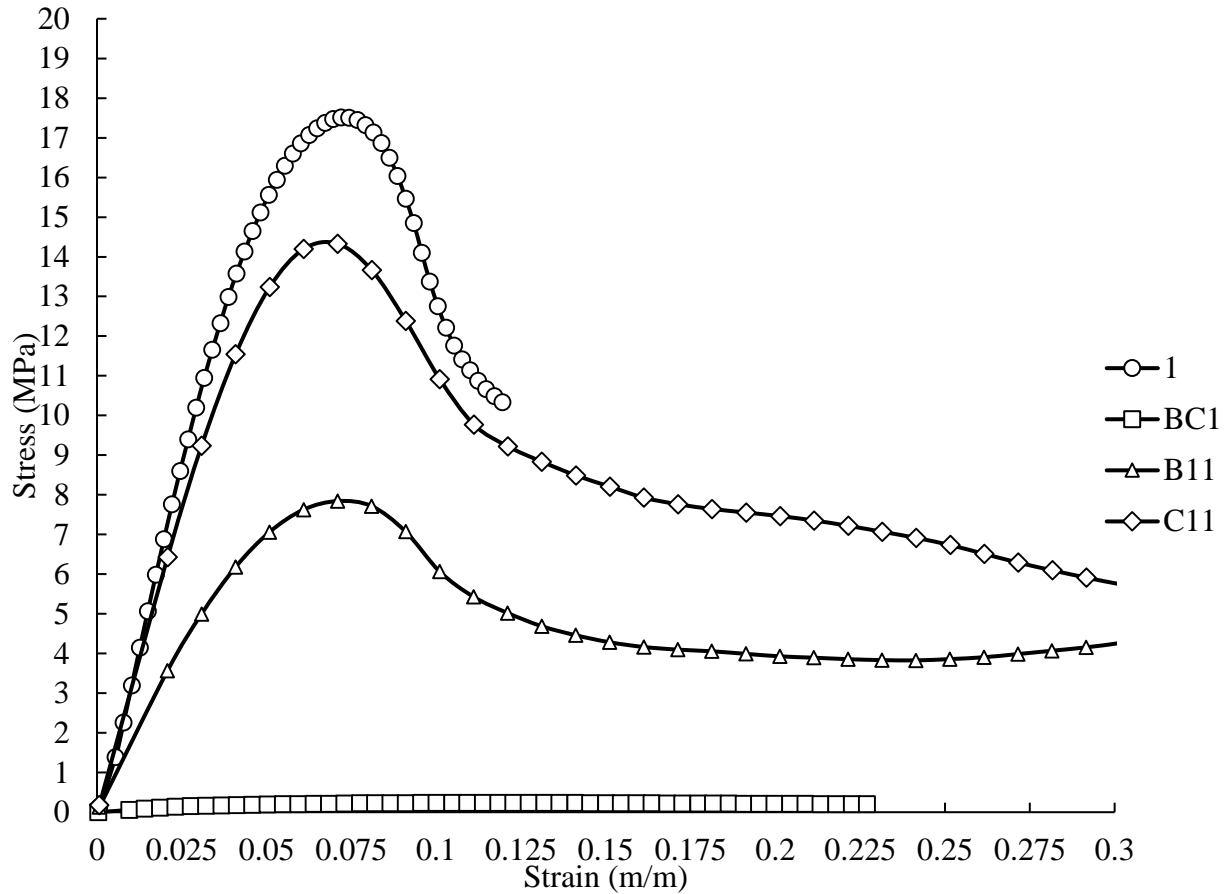


Figure 41: Material comparison Stress vs. Strain.

The following

Table 13 is the calculated values of specific strength, ultimate stress, and is the calculated young's modulus values for all the methods. The Figure 42, Figure 43, and Figure 44 below are the graphical representation of the ultimate stress, young's modulus, and specific strength respectively for all methods and materials. Some of the graphs and tables also include Mild Steel ANSI 1045 as indicators for comparison of the materials. The values of the Mild Steel ANSI 1045 were pulled from engineering toolbox (Engineering Toolbox, 2008).

Table 13: Sample Results

Sample	Specific Strength (MPa m ³ /kg)	Ultimate Strength (MPa)	Young's Modulus (MPa)
Pre1	0.066	7.975	147.77
Pre2	0.062	7.831	149.88
Pre3	0.061	8.166	146.04
Pre4	0.065	8.083	147.10
1A1	0.075	10.06	162.27
2B1	0.063	8.340	152.01
1C2	0.075	9.977	173.83
2D2	0.060	8.061	149.97
10A	0.013	7.741	233.44
10B	0.016	9.172	233.59
10C	0.012	6.832	235.21
10D	0.014	8.276	234.41
5A	0.015	8.540	249.41
5B	0.014	8.044	225.79
5C	0.016	9.063	225.60
5D	0.013	7.808	222.83
Old1	0.066	7.975	147.77
Old2	0.062	7.831	149.88
New1	0.033	4.868	49.03
New2	0.035	4.780	41.24
ST1	0.036	5.014	126.67
ST2	0.033	4.493	121.67
ST3	0.051	7.902	173.40
ST4	0.051	7.605	164.48
1	0.097	17.73	388.75
2	0.109	18.25	399.74
3	0.099	17.52	389.30
4	0.103	17.51	392.23
BC1	0.013	0.297	6.05
BC2	0.013	0.298	6.32
PC1	0.008	0.200	4.24
PC2	0.009	0.199	4.76
B11	0.047	7.849	142.70
B22	0.052	8.709	167.42
B33	0.049	8.260	159.88
C11	0.075	14.37	279.84

C22	0.078	15.03	284.86
C33	0.073	13.98	287.66
ANSI 1045	0.073	585	205000

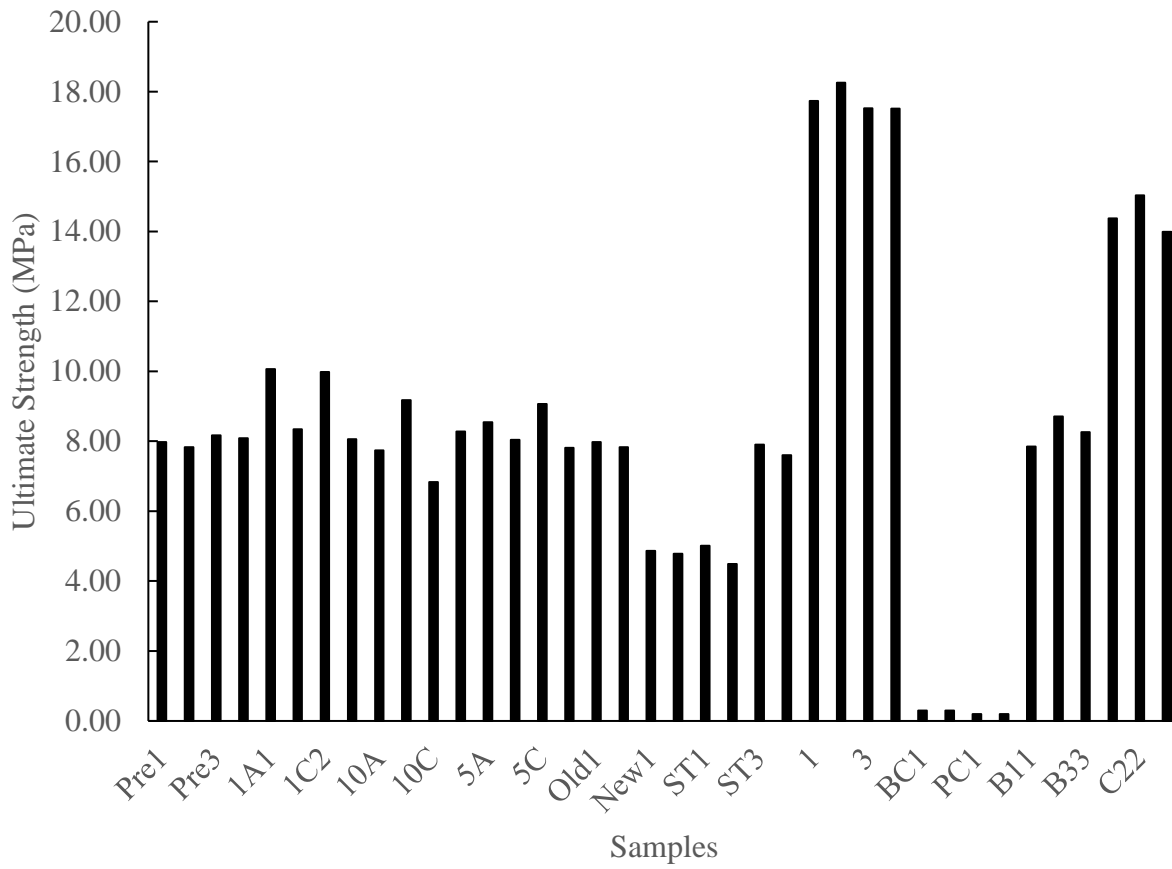


Figure 42: Ultimate Strength Bar Graph

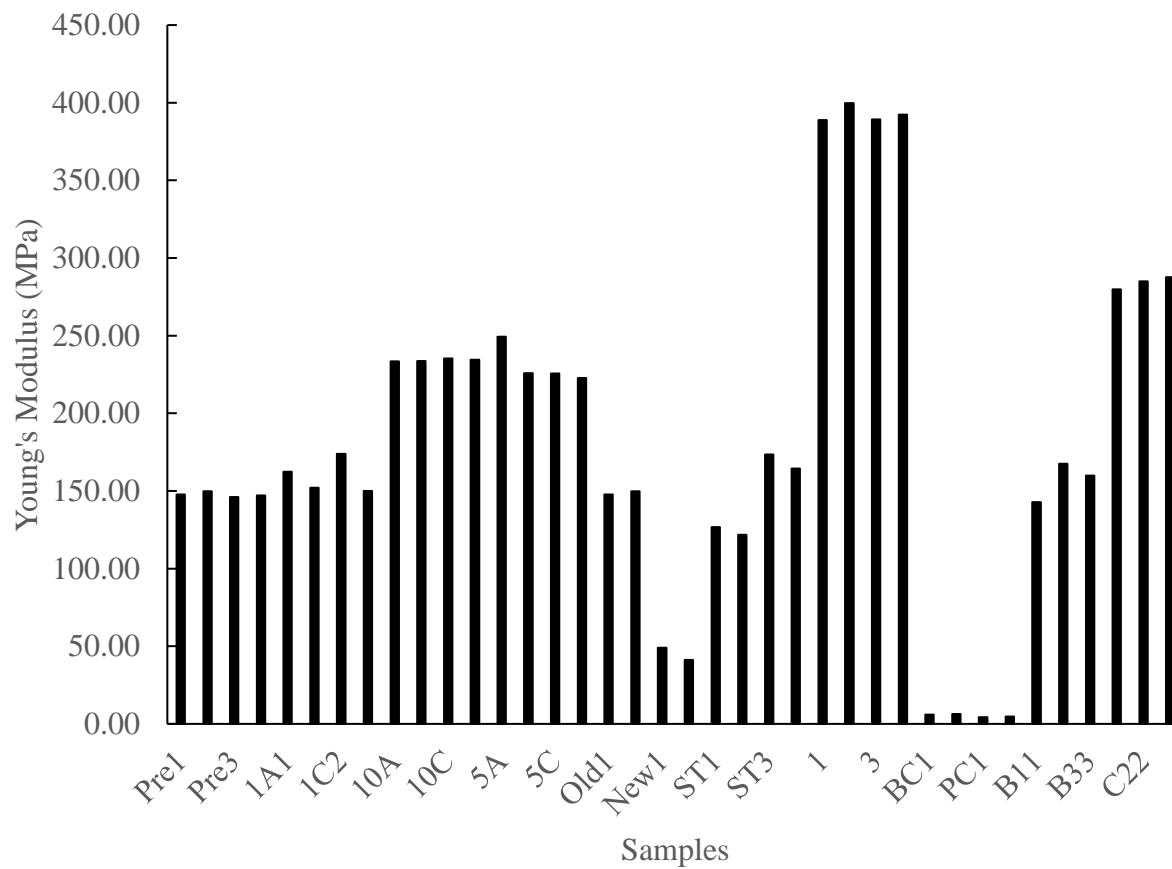


Figure 43: Young's Modulus Bar Graph

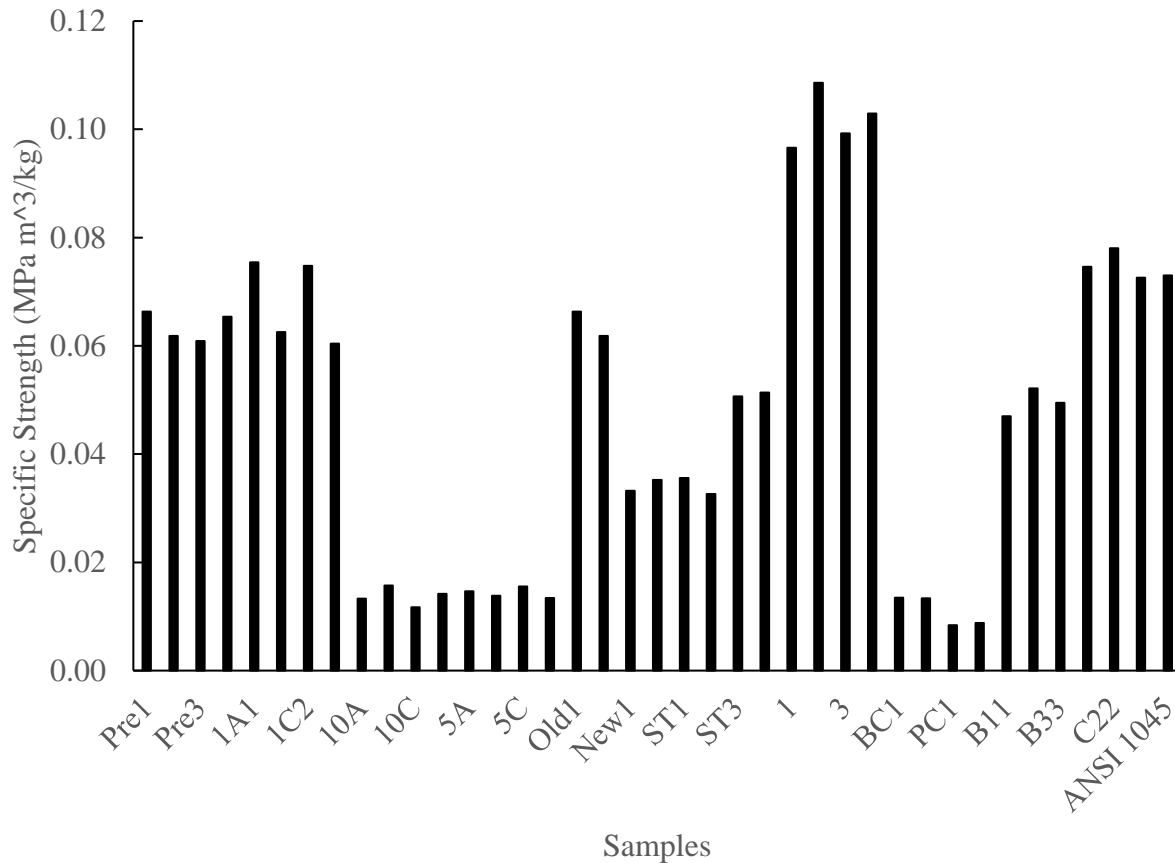


Figure 44: Specific Strength Bar Graph

4.4 Statistical Analysis:

Standard deviation (SD) is calculated by finding summation of the absolute value of the square of the value represented by X subtracted by the Mean denoted by U. Then divided by the sample size minus one, and taking the square root of all of that, which can be seen in Equation 7. Then the 95% confidence interval is determined by 1.96 times the standard deviation.

$$SD = \sqrt{\frac{\sum |X - U|^2}{n - 1}}$$

Equation 7

$$95\% \text{ Confidence} \\ = 1.96 * SD$$

Equation 8

The following Table 14, Table 15, and Table 16 is the standard deviation and 95% confidence interval data statistical analysis for the ultimate strength, Young's Modulus, and specific strength.

Table 14: Ultimate Strength Statistical Analysis

Sample	Ultimate Strength (MPa)	Ultimate Strength Standard Deviation	95% Confidence
Optimized	17.7578	0.3481	0.6823
Control	8.2727	0.4304	0.8436
Final Product	14.4657	0.5287	1.0362
Bar Cooled	0.2975	0.0007	0.0013
Pool Cooled	0.1994	0.0011	0.0021

Table 15: Young's Modulus Statistical Analysis

Sample	Young's Modulus (MPa)	Young's Modulus Standard Deviation	95% Confidence
Optimized	392.5038	5.0582	9.9141
Control	156.6671	12.6697	24.8327
Final Product	284.1230	3.9634	7.7682
Bar Cooled	6.1830	0.1901	0.3727
Pool Cooled	4.5023	0.3714	0.7279

Table 16: Specific Strength Statistical Analysis

Sample	Avg. Specific Strength (MPa m ³ /kg)	Specific Strength Standard Deviation	95% Confidence
Optimized	0.1018	0.0052	0.0102
Control	0.0495	0.0495	0.0971
Final Product	0.0751	0.0751	0.1471
Bar Cooled	0.0134	0.0001	0.0002
Pool Cooled	0.0086	0.0003	0.0005

Using the 95% confidence interval and applying it to the mean values. One can determine the upper and lower limits of the samples sets as shown below in the following figures. Figure 45, Figure 46, and Figure 47, are the Bar graphs that display the materials average Ultimate strength, Young's Modulus, and Specific Strength respectively. These graphs display the average values for the Optimized data set, the Control, Final Product, and Bar and Pool cooling methods for the cellulose. The graphs have errors bars to display the variance internal of the data series.

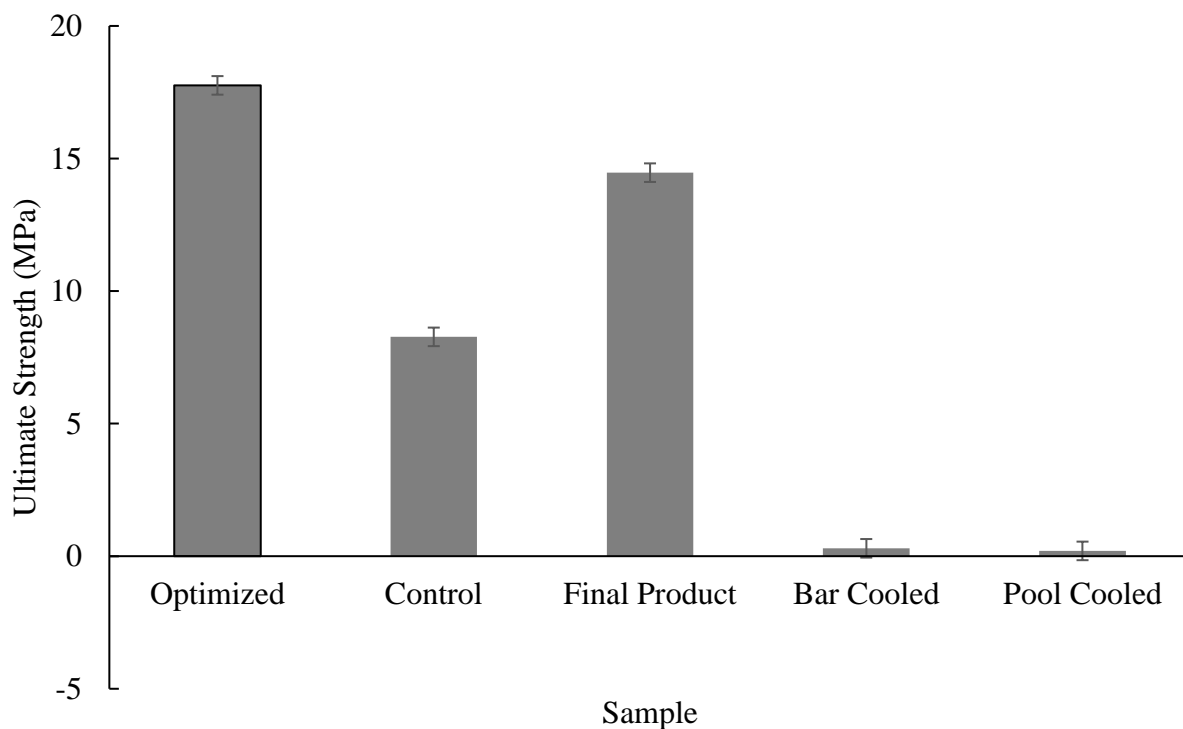


Figure 45: Ultimate Strength Materials Avg.

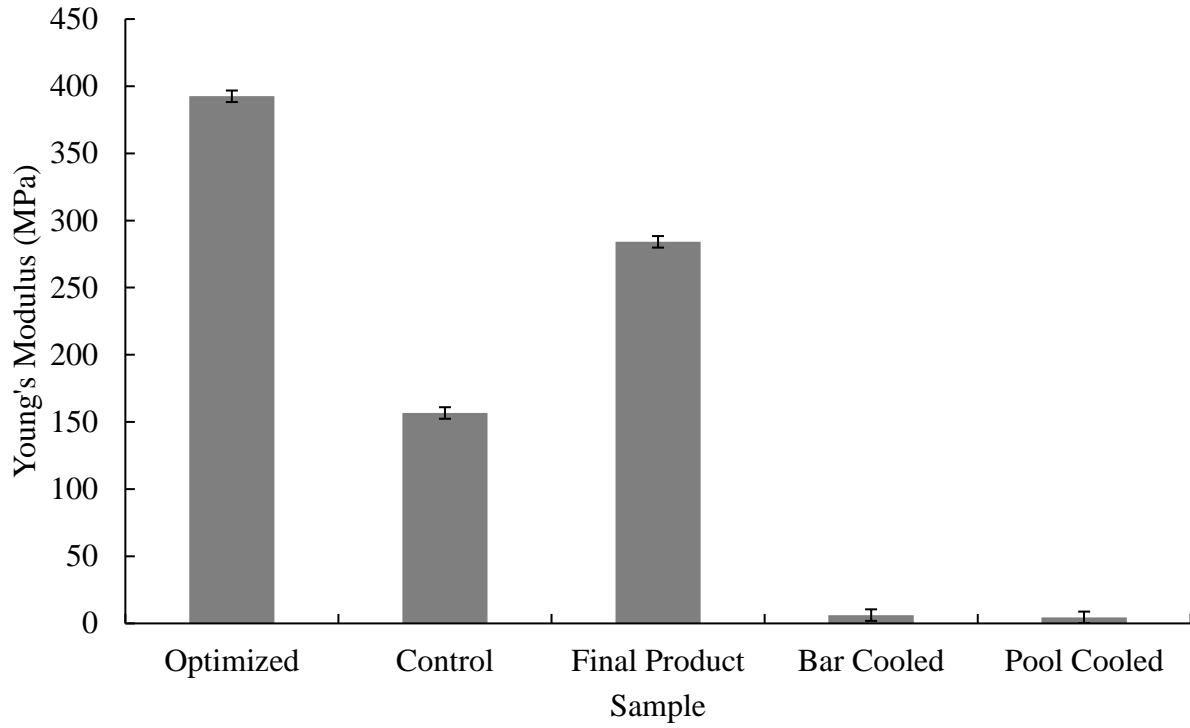


Figure 46: Young's Modulus Materials Avg.

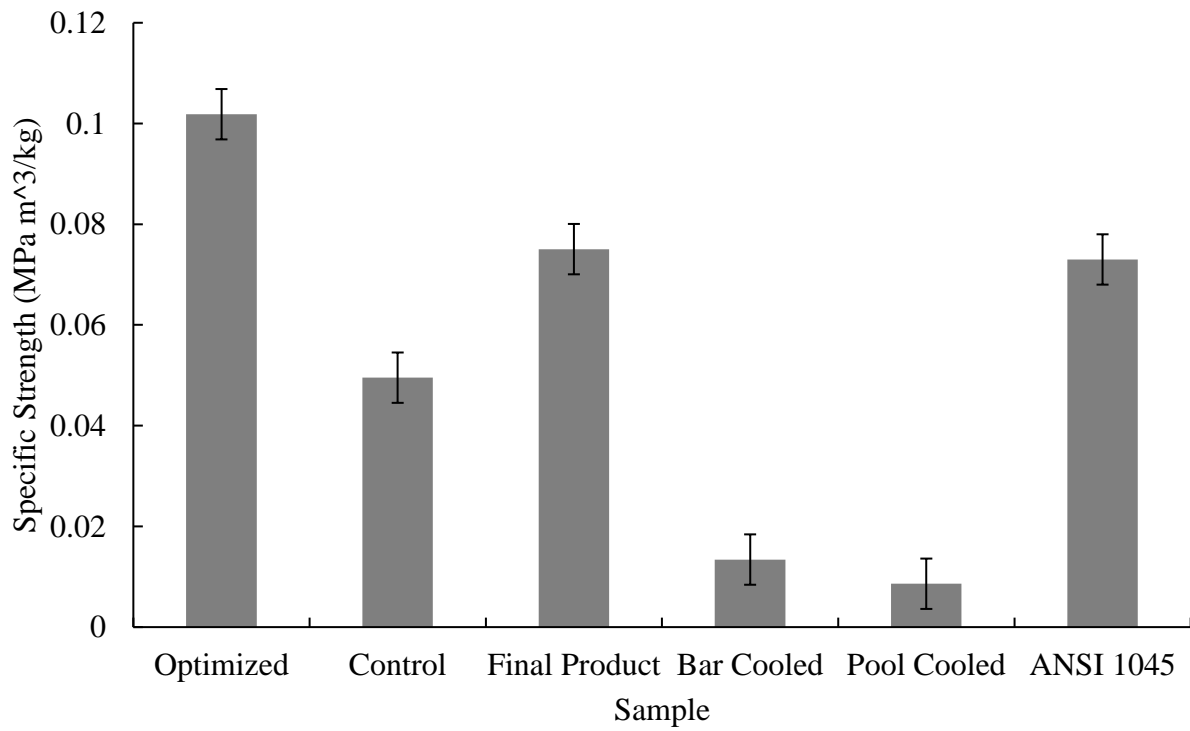


Figure 47: Specific Strength Materials Avg.

The following Figure 48, Figure 49, and Figure 50 graphs are the average Stress vs. average Strain for the Optimized, Control, and Final Product data series, respectively. These stress vs. strain curves, have upper and lower limits plotted as well, these limits are using the 95% confidence interval calculated using Equations 7 and 8. The average stress and strain for the following figures were calculated by taking the average of a single stress/strain point for the multiple data sets, then calculating the standard deviation for that individual point and applying the 95% confidence interval to the mean to create the upper and lower limit curves based for each point. This shows that the data is more randomized after the buckling of the compression sample as the variance increases, and is predictable after the initial buckling and becomes consistent to create a tough curve.

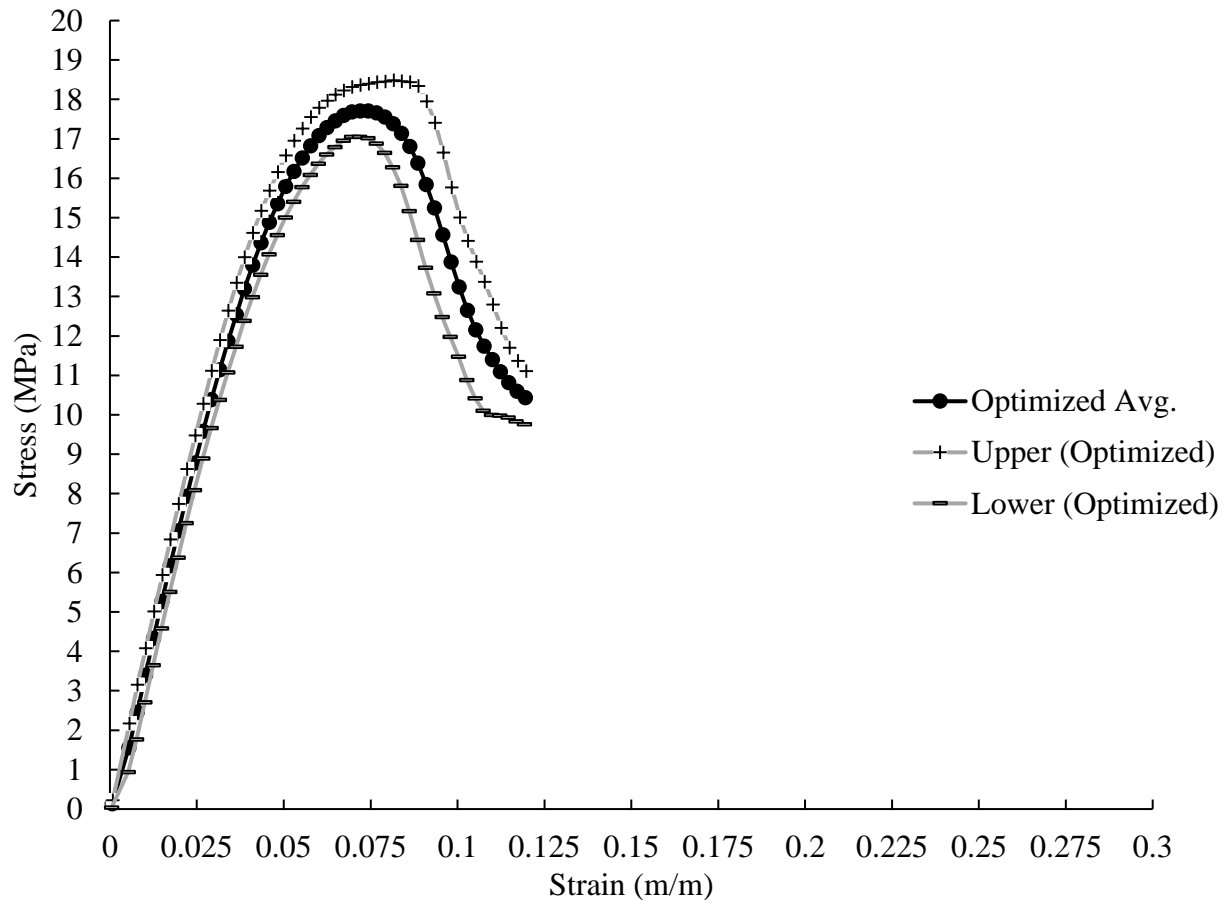


Figure 48: Optimized Avg.

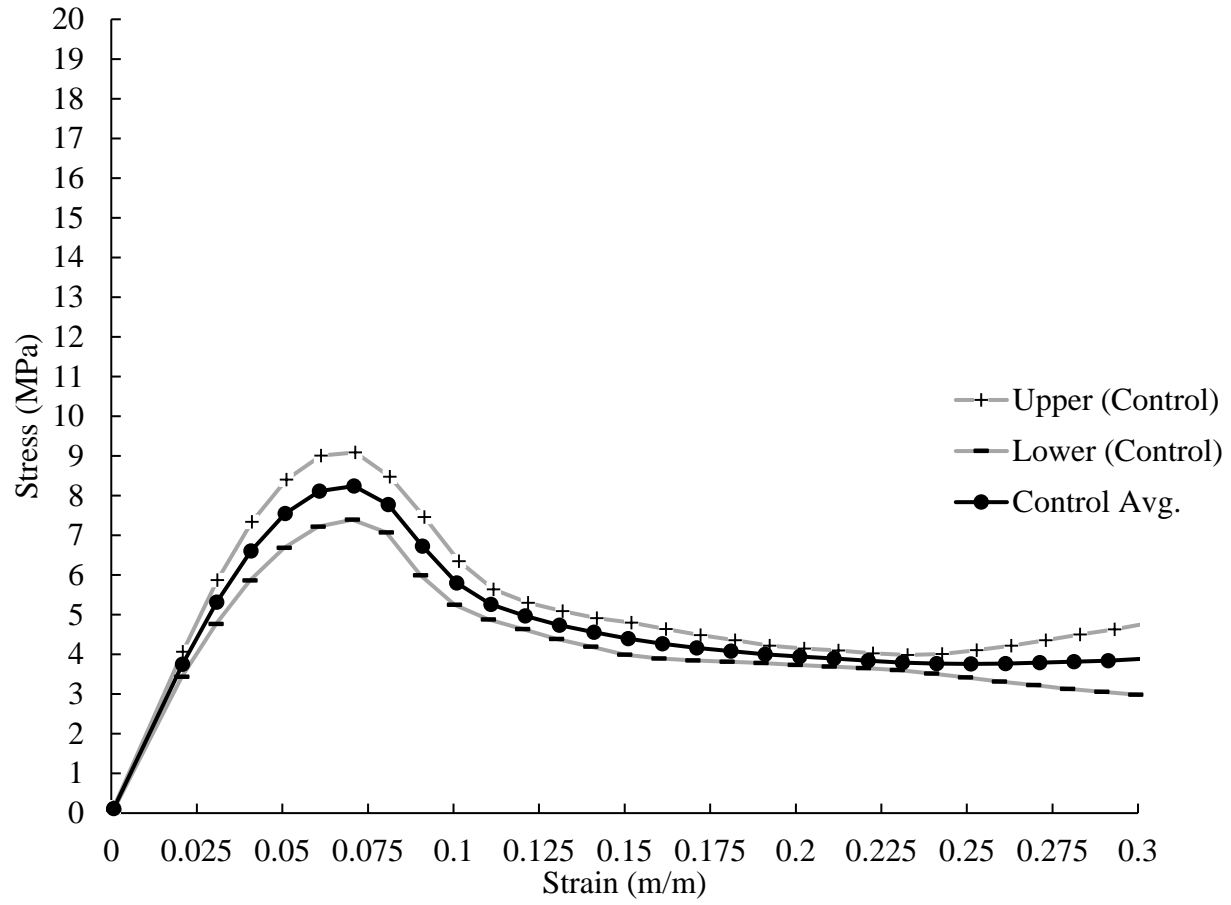


Figure 49: Control Avg.

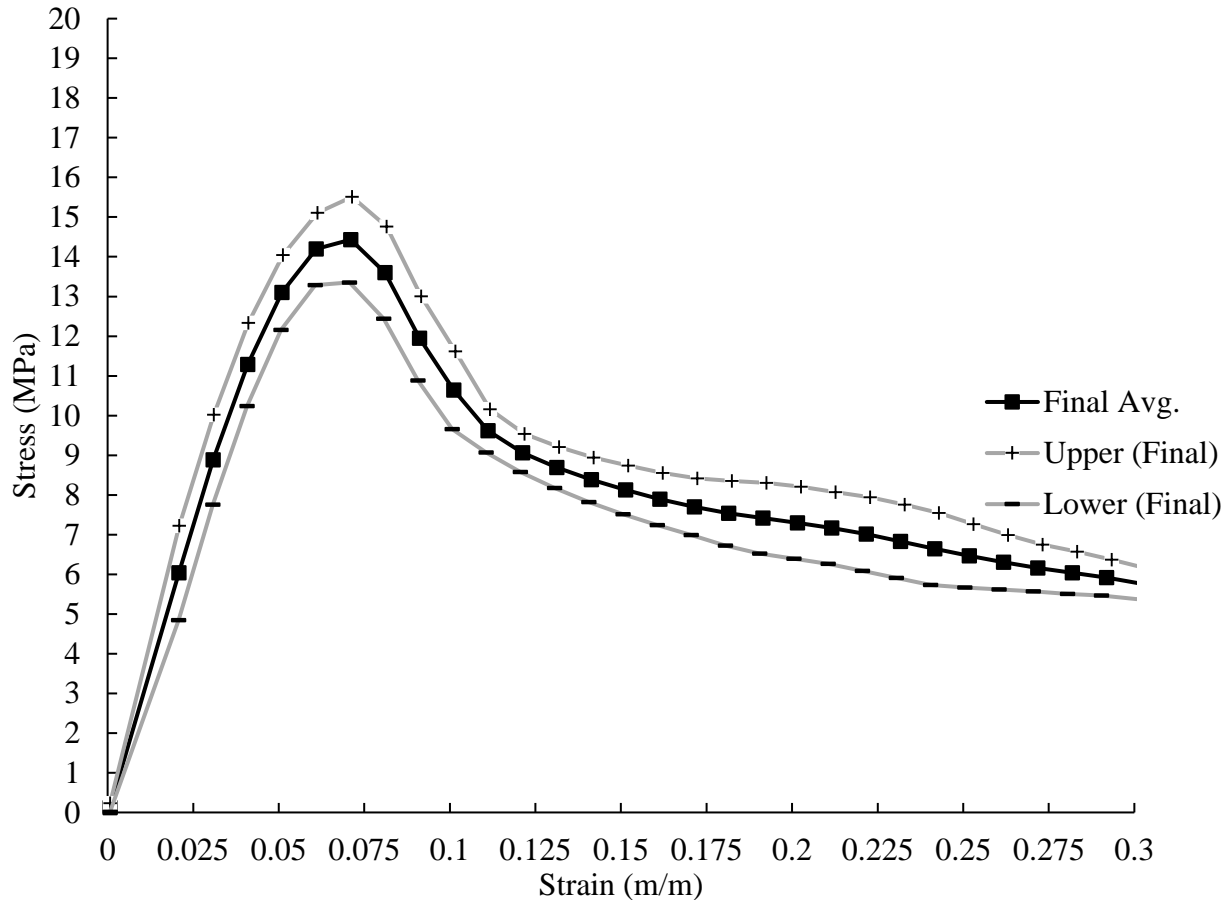


Figure 50: Final Product Avg.

4.5 Discussion:

The determining factor of this study was the specific strength of the material produced. This factor is calculated using the density and stress of the material. Specific strength is the force per unit area at failure divided by the density. The most common understanding is strength to weight ratio. In this experiment a unit cell mimicking the lattice structure of diamond. This unit cell was repeated in every direction, to create a 3D structure this structure was then optimized and cut into a cylindrical shape with dimensions of 50mm high and 19mm diameter. The samples shape and these dimensions were chosen to be able to observe a uniform stress across the compression test. The sample was then printed on a Form 2, using a UV resin called Tough V2 provided by Formlabs. Following their recommendations for processing the material the stress vs.

strain values observed in Figure 16. One can see that there are inconsistencies in the curves, the yield points, and extreme differences in mass from Table 2. These values were also proportional low to other materials with the same characteristics such as ABS plastic as that is what the Tough V2 resin was said to resemble.

There was a decision to look closer at the process, so all the variables that could affect the strength were observed and removed accordingly. The sample placement in the curing chamber was studied this revealed that if the was sample placed in the front such as 2B1 and 2D2, the ultimate strength values of 8.340MPa and 8.061MPa, was consistently lower than that of 1A1 and 1C2 with values of 10.060MPa and 9.977MPa respectively. So, the decision for all samples were then cured in the back and made sure to rotate the samples as necessary in the chamber, was made.

The next study was done on the IPA time 4 samples at 10 minutes and 5 samples at 5 minutes. These samples showed that the IPA affected the stiffness value or Young's Modulus of the material. The 5-minute samples 5A-5D were more consistent, as 10A-10D were scattered. The IPA time was further tested qualitatively by checking the rigidity and swelling of the material shown in Table 5 the sample T_1 was the closest to the control. The decision was made to reduce the IPA time to be below 30 seconds to ensure that the IPA was not affecting the materials performance in a negative manner.

The chamber selection was the next variable with the values being much lower than anticipated. The use of a 405nm UV light should produce optimal results as this frequency matches that of the laser that cures the structure in the 3D printer. A chamber was created using the 405nm wavelength LED's it produced very low values with we believed was due to the intensity of the LED's compared to the blub in the 365nm chamber. With time constraints considered the choice to remain using the 365nm wavelength chamber was made. The supporting results can be seen in

Figure 19 with the Old1 and Old2 being 4 times greater in ultimate stress values and having a significantly higher young's modulus of 147.77MPa for the Old1 and 49.03MPa for the New1 respectively.

Sample set time was next as the process was lengthy and difficult to be in the laboratory as the samples finished curing each time so the assumption was that the lower amount of time the samples set the higher the moisture content or the effect of the residual IPA on the material. One set was allowed to set for one day and the other for one hour. Their respective ultimate stress values recorded were 5.014MPa for ST1 and 7.902MPa for ST3 this is a 3MPa increase just by testing the sample at an earlier time. This discovery led to the decision of creating a control sample beside the final product to ensure the values were comparable.

After taking these variables into consideration the samples were reprocessed with greater care following the new decisions. The resulting stress versus strain curves for this trial can be seen in Figure 22 above. The peak values were much greater than any of the other methods, the values of young's modulus, ultimate strength, and specific strength can be seen in Table 13. This was chosen as the method to continue the research with.

Next was to determine how the addition of the cellulose fibers would be introduced. The cellulose was testing two ways as previously mentioned, Pool cooling and Bar cooling. Bar cooling was the overall better method for our application as the ultimate strength for BC1 was 0.297MPa, and PC1 was 0.200. The young's moduli for these were 6.05MPa and 4.24MPa respectively. It also to take account for the increase in specific strength of $0.013\text{MPa}\cdot\text{m}^3/\text{kg}$ for BC1 and $0.008\text{MPa}\cdot\text{m}^3/\text{kg}$ for PC1. After evaluating these numbers, better choice was to use the Bar cooling method to carry forward in combination of the materials for the compression tests. It was however important to observe the microstructure of these two methods to understand the changes

to the structure in the two types of cooling. Looking at the Figures 26-29 for the Pool cooled sample, one can take note that the structure of is the same in the cross section and the axial direction proving that the assumption of uniform cooling from the outside in occurred, creating a more homogeneous material. Looking at the Bar cooled structure in Figures 30-33, it can be noted the cross section is similar to that of the Pool cooling, yet less dense with fibers. The axial direction can clearly be seen to have elongated fibers running the length of the sample. This is an indication that the fibers were cured causing a bonding to happen creating a heterogenous structure. Further microstructure study was taken using an electron microscope (SEM) to observe the material at x200, x400, and x2000 magnifications shown in Figures 34, 35, and 36 respectively. The samples of Bar cooling and Pool cooling were indistinguishable on these magnifications. One can notice that the fibers are randomized and the structures are very porous from the voids left by the ice casting process.

The struggling to get consistency in the material properties with the Tough V2 material was mainly, because of its sensitivity to light, moisture, and time degradation. This made the processing of the material on a multi-scale level difficult to be completed. Other plastics also have a shelf life, like nylon climbing ropes must be retired after so many hours in UV light. It is understandable there will be some degradation in these samples, but the speed of which it happens seems to be amplified with this material, Tough V2. After adjusting the process, the combination of the two materials could begin. Three sets of the 3D printed structure were printed and processed, three of these were set aside as control samples since set time before testing was important to control. The other three samples were filled with the cellulose fibers and ice casted using the Bar cooling method. The samples took three days to process. The control and final product were tested producing expected results. The data was then statistically analyzed on a 95% confidence interval.

The average stress and strain for the following figures were calculated by taking the average of a single stress/strain point for the multiple data sets, then calculating the standard deviation for that individual point and applying the 95% confidence interval to the mean to create the upper and lower limit curves based for each point. This shows that the data is more randomized after the buckling of the compression sample as the variance increases, and is predictable after the initial buckling and becomes consistent to create a tough curve. Using the averages the final product had an increase in specific strength of 1.52 times with average control value of $0.0495 \text{ MPa}\cdot\text{m}^3/\text{kg}$ to final product value of $0.0750 \text{ MPa}\cdot\text{m}^3/\text{kg}$. An increase in ultimate strength and young's modulus also occurred. Ultimate strength increased 1.75 times from 7.849MPa to 14.375MPa and Young's modulus almost doubled at 1.8 times increase from 156.66MPa to 284.12MPa respectively. It is noticeable that the overall increase in strength of the material. These results shown in Table 13, were proof that the creation of the material in a hierarchical fashion would produce and overall increase in the materials properties. The cellulose structure was able to help support the 3D printed truss system to affect the characteristics much light bamboo's fibers are supported by its foam like matrix. Overall this research was a success in proving the hypothesis.

CHAPTER 5: CONCLUSIONS

5.1 Conclusions:

The method of processing the Tough V2 material should continue to further adjust and account for the irregularities for this research, but the overall goal was achieved. The Tough V2 material degrades by time and accounts for the irregularities in this research, and this was overcome using a control sample with the final product. Proof that the creation of the material in a hierarchical fashion would produce an overall increase in material properties can be seen. The control and final product were tested producing expected results as the final product had an increase in specific strength of 1.75 times with average control value of $0.0495 \text{ MPa}\cdot\text{m}^3/\text{kg}$ to final product value of $0.0750 \text{ MPa}\cdot\text{m}^3/\text{kg}$. An increase in ultimate strength and young's modulus also occurred. Ultimate strength increased 1.75 times from 7.849MPa to 14.375MPa and Young's modulus almost doubled at 1.8 times increase from 156.66MPa to 284.12MPa respectively. It is noticeable that the overall increase in strength of the material these results shown in Table 13, were proof that the creation of the material in a hierarchical fashion would produce and overall increase in the materials properties. Yeah and then I was like... done.

5.2 Recommendations:

The recommendations for future work would be to conduct the same study on a more reliable less reactive material provided from FormLabs. The High Temp material would be a perfect choice due to its low expansion rates to different chemicals, as the Tough V2 material expands with water and cracks with acetone. The Tough V2 is unable to be used for further testing with a third layer of material in the Nano scale since Macro and Micro are the focus of this research. The next recommendation for this research would be work on creating a smaller more optimized model for 3D printing for expedited printing and curing times while wasting less material. Also, the creation of a working 405nm UV curing chamber would be beneficial. The final recommendation for this research is to have a complete simulation study conducted on these micro

truss systems to better understand the micro-buckling and structure buckling happening in these models.

REFERENCES

- [1] "AM Basics." Additive Manufacturing (AM). <http://additivemanufacturing.com/basics/>.
- [2] A. Al-Sawalmih, C. Li, S. Siegel, H. Fabritius, S. Yi, D. Raabe, P. Fratzl, O. Paris, *Adv. Funct. Mater.* 2008, 18, 3307.
- [3] A. R. Studart, *Chem. Soc. Rev.* 2016, 45, 359.
- [4] C. Sachs, H. Fabritius, D. Raabe, *J. Mater. Res.* 2006, 21, 1987.
- [5] C. Sachs, H. Fabritius, D. Raabe, *J. Struct. Biol.* 2006, 155, 409.
- [6] E. Degtyar, M. J. Harrington, Y. Politi, P. Fratzl, *Angew. Chem., Int. Ed.* 2014, 53, 12026.
- [7] E. Munch, M. E. Launey, D. H. Alsem, E. Saiz, A. P. Tomsia, R. O. Ritchie, *Science* 2008, 322, 1516.
- [8] Engineering ToolBox, (2008). *Engineering Materials*.
https://www.engineeringtoolbox.com/engineering-materials-properties-d_1225.html
- [9] F. Barthelat, H. D. Espinosa, *Exp. Mech.* 2007, 47, 311.
- [10] F. Barthelat, H. Tang, P. D. Zavattieri, C. M. Li, H. D. Espinosa, *J. Mech. Phys. Solids* 2007, 55, 306.
- [11] F. Barthelat, Z. Yin, M. J. Buehler, *Nat. Rev. Mater.* 2016, 1, 16007.
- [12] G. Mayer, *Science* 2005, 310, 1144.
- [13] H. B. Yao, H. Y. Fang, X. H. Wang, S. H. Yu, *Chem. Soc. Rev.* 2011, 40, 3764.
- [14] H. B. Yao, J. Ge, L. B. Mao, Y. X. Yan, S. H. Yu, *Adv. Mater.* 2014, 26, 163.
- [15] H. D. Espinosa, J. E. Rim, F. Barthelat, M. J. Buehler, *Prog. Mater. Sci.* 2009, 54, 1059.
- [16] H. O. Fabritius, C. Sachs, P. R. Triguero, D. Roobe, *Adv. Mater.* 2009, 21, 391.
- [17] Hibbleler, R. C.
<https://docs.google.com/file/d/0B0uVd31B7zGEBjRnWE5qdnZBWjA/edit>.
- [18] J. F. Vincent, U. G. Wegst, *Arthropod Struct. Dev.* 2004, 33, 187.
- [19] J. S. Peng, Q. F. Cheng, *Adv. Mater.* 2017, 29, 1702959.
<https://doi.org/10.1002/adma.201702959>

- [20] J. Wang, L. Lin, Q. Cheng, L. Jiang, *Angew. Chem., Int. Ed.* 2012, 51, 4676.
- [21] L. B. Mao, H. L. Gao, H. B. Yao, L. Liu, H. Colfen, G. Liu, S. M. Chen, S. K. Li, Y. X. Yan, Y. Y. Liu, S. H. Yu, *Science* 2016, 354, 107.
- [22] L. Qiu, J. Z. Liu, S. L. Chang, Y. Wu, D. Li, *Nat. Commun.* 2012, 3, 1241.
- [23] M. A. Meyers, J. McKittrick, P. Y. Chen, *Science* 2013, 339, 773.
- [24] M.-M. Giraud-Guille, H. Chanzy, R. Vuong, *J. Struct. Biol.* 1990, 103, 232.
- [25] Obataya, Eiichi, Peter Kitin, and Hidefumi Yamauchi. *Wood Science and Technology* 41, no. 5 (2007): 385-400. doi:10.1007/s00226-007-0127-8.
- [26] P. Ming, Z. F. Song, S. S. Gong, Y. Y. Zhang, J. L. Duan, Q. Zhang, L. Jiang, Q. F. Cheng, *J. Mater. Chem. A* 2015, 3, 21194.
- [27] Q. Cheng, L. Jiang, Z. Tang, *Acc. Chem. Res.* 2014, 47, 1256.
- [28] R. Minke, J. Blackwell, *J. Mol. Biol.* 1978, 120, 167.
- [29] S. J. Wan, J. S. Peng, Y. C. Li, H. Hu, L. Jiang, Q. F. Cheng, *ACS Nano* 2015, 9, 9830.
- [30] S. Keten, Z. Xu, B. Ihle, M. J. Buehler, *Nat. Mater.* 2010, 9, 359.
- [31] S. Nikolov, M. Petrov, L. Lymperakis, M. Friak, C. Sachs, H. O. Fabritius, D. Raabe, J. Neugebauer, *Adv. Mater.* 2010, 22, 519.
- [32] S. Wan, J. Peng, L. Jiang, Q. Cheng, *Adv. Mater.* 2016, 28, 7862.
- [33] S. Weiner, W. Traub, H. D. Wagner, *J. Struct. Biol.* 1999, 126, 241.
- [34] U. G. Wegst, H. Bai, E. Saiz, A. P. Tomsia, R. O. Ritchie, *Nat. Mater.* 2015, 14, 23.
- [35] U. Wegst, M. Ashby, *Philos. Mag.* 2004, 84, 2167.
- [36] Wohlers, Terry, and Tim Gornet. Wohlersassociates.com. 2014. Accessed April 23, 2017. <http://wohlersassociates.com/history2014.pdf>.
- [37] Xu, Mitra, Miguez, Mayfield, Shinall, Bessenbacher, Davis, Spratlin. *Mechanics of Biological Systems and Materials*, Volume 6, chapter 10, page 67-74
- [38] Y. Bouligand, *Tissue Cell* 1972, 4, 189192.
- [39] Y. Liu, Z. Xu, J. Zhan, P. Li, C. Gao, *Adv. Mater.* 2016, 28, 7941.

- [40] Y. S. Kim, M. Liu, Y. Ishida, Y. Ebina, M. Osada, T. Sasaki, T. Hikima, M. Takata, T. Aida, *Nat. Mater.* 2015, 14, 1002.
- [41] Y. Zhang, S. Gong, Q. Zhang, P. Ming, S. Wan, J. Peng, L. Jiang, Q. Cheng, *Chem. Soc. Rev.* 2016, 45, 2378.
- [42] Y. Zhang, Y. Li, P. Ming, Q. Zhang, T. Liu, L. Jiang, Q. Cheng, *Adv. Mater.* 2016, 28, 2834.
- [43] Z. An, O. C. Compton, K. W. Putz, L. C. Brinson, S. T. Nguyen, *Adv. Mater.* 2011, 23, 3842.
- [44] Zhang, Xiaoping, Fang Wang, and Leon Keer. *Materials* 8, no. 10 (2015): 6597-608. doi:10.3390/ma8105327.